TI Designs: TIDA-01596
スマート・サーモスタットでの周囲温度検出用の局所化された熱補償のリファレンス・デザイン

TEXAS INSTRUMENTS

概要

このリファレンス・デザインは、排気空間近くで周囲温度検出が不正確になる主な原因である、局所的なサーモスタットの熱生成に対処します。この誤差は最終的にHVACサイクルのオーバーシュートを引き起こし、エネルギー料金の増大を招きます。PCB上に、低コストのアナログ温度センサのネットワークを使用することで、内部的なサーモスタットの温度勾配を検出し、効果的に補償して、実際の周囲温度の値を得ることができます。その後で、外部のアナログ出力温度センサを、ウィンドウ・コンパレータが内蔵され、ヒステリシスをプログラム可能な、ナノパワーのアナログ/デジタル・コンバータに接続することで、温度の範囲外状況を自律的に監視できます。

リソース

TIDA-01596	デザイン・フォルダ
CC3220	プロダクト・フォルダ
TMP235	プロダクト・フォルダ
INA230	プロダクト・フォルダ
ADS7142	プロダクト・フォルダ
LMT84	プロダクト・フォルダ

E2E™エキスパートに質問

特長

- 低コスト、ナノパワーのセンサ・モニタと、アナログ出力の温度センサを組み合わせ、自律的に温度を正確にデジタル値に変換
- 電流シャント・モニタを使用して、メイン電源の電流および電力を監視
- 2つの温度センサ・デバイスの組により、基板上での温度勾配を判定
- 局所的な熱の生成のため20Ωの電力抵抗を使用
- BoosterPack™プラグイン・モジュールのエコシステムと互換性を持つヘッダーを使用して設計され、ソフトウェアはCC3220ワイヤレスMCU LaunchPad™で動作するよう設計

アプリケーション

- サーモスタット
- HVACシステム・コントローラ
- ワイヤレス環境センサ

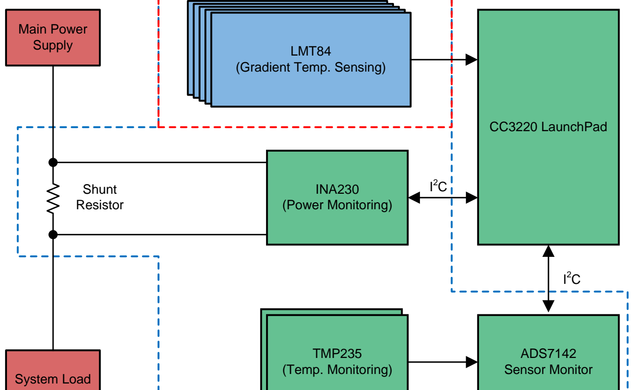

Copyright © 2018, Texas Instruments Incorporated

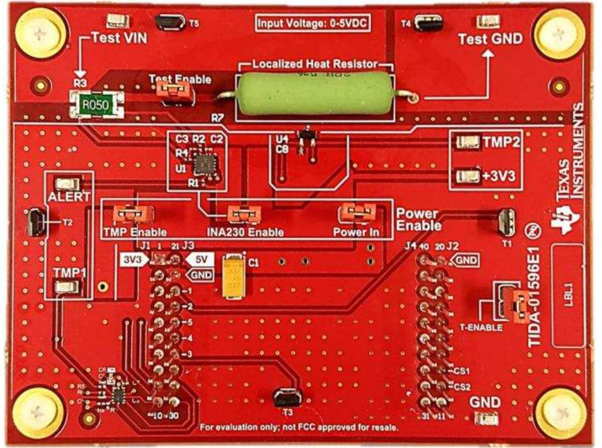

TIDUDO1 翻訳版 — 最新の英語版資料 http://www-s.ti.com/sc/techlit/TIDUDO1
Copyright © 2018, Texas Instruments Incorporated

使用許可、知的財産、その他免責事項は、最終ページにあるIMPORTANT NOTICE(重要な注意事項)をご参照くださいますようお願いいたします。英語版のTI製品についての情報を翻訳したこの資料は、製品の概要を確認する目的で便宜的に提供しているものです。該当する正式な英語版の最新情報は、www.ti.comで閲覧でき、その内 容が常に優先されます。TIでは翻訳の正確性および妥当性につきましては一切保証いたしません。実際の設計などの前には、必ず最新版の英語版をご参照くださいますようお願いいたします。

1 System Description

As technology continues to thrive in the HVAC industry, more devices are increasing their capabilities and energy consumption. One issue seen in newer "smart" thermostats is that their increased capabilities come at the expense of erroneous ambient temperature readings due to heat dissipation caused by additional circuitry. Over time, these seemingly small offsets between the set temperature and the actual satisfied temperature where the unit turns off can cost more than expected. As the temperature in a home or industrial setting reaches the target temperature, the change in temperature becomes much less influenced from the air handlers cool or warm air supply. This lack of influence is due to the properties of thermodynamics and the non-linear rate of heat energy absorption associated with these principles.

This reference design incorporates the INA230, ADS7142, TMP235, and the LMT84 devices, allowing the design many different combinations to provide accurate ambient temperature results. The TMP235 analog temperature sensors offer a very accurate temperature reading while maintaining a low cost for cost-sensitive designs. These devices are combined with the ADS7142 nano-power sensor monitor to provide a solution to fit any design with high accuracy and low cost. The LMT84 devices provide the capability of accurately measuring the convective heat transfer by being mounted slightly elevated from the surface of the PCB, providing an alternative low-cost temperature offset compensating solution. The INA230 provides additional crucial data pertaining to the current and power consumption of the system as a whole, a leading indicator for heat generation. Combined, these sensors work as a network in place of a single sensor design and can increase accuracy of the algorithms beyond that specified for a particular device.

1.1 Key System Specifications

表 1. Key System Specifications

PARAMETER	SPECIFICATIONS	DETAILS
Power supply voltage	0 V to 5 V	2.4
Average on-state current consumption	469.64 µA at 71.6°C	3.2.2.3
Accuracy of convective temperature sensor	±0.667°F	3.2.2.2.3
Accuracy of surface temperature sensor	±1°F	3.2.2.2.2
Combined accuracy of current and temperature sensor	< 1°F	3.2.2.2.1
Current sense accuracy	< 0.60% error	2.3.3
Testing load current	0 mA to 250 mA	
Allowable load temperature variation	0°C to 19°C (based on input voltage)	2.4.5.3

Copyright © 2018, Texas Instruments Incorporated

2 System Overview

2.1 Block Diagram

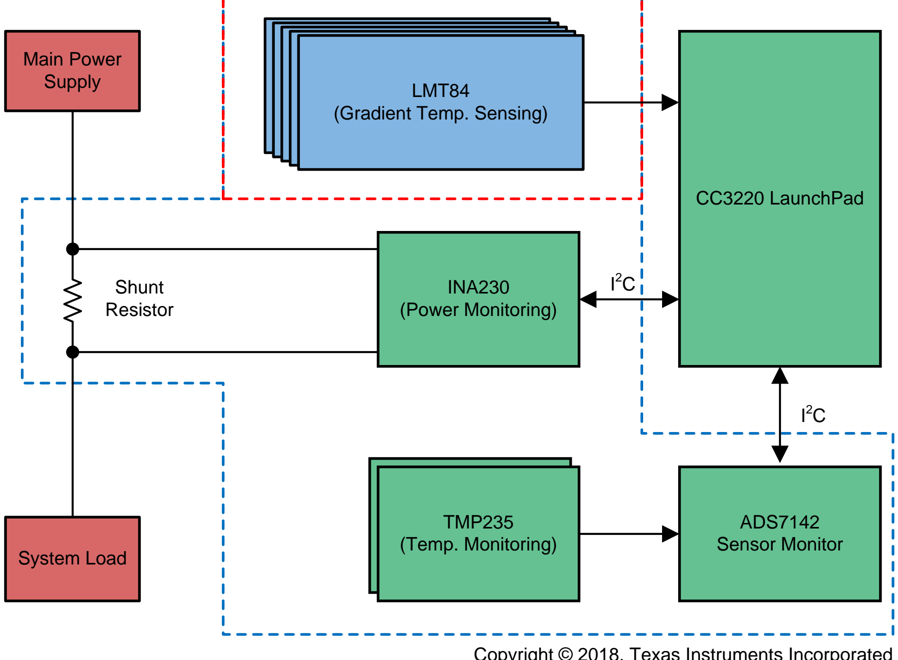

図 1. TIDA-01596 Block Diagram

2.2 Design Considerations

As with any temperature compensation design, the environment plays an important role in the behavior of the device thermodynamics and, consequently, the ability of the temperature compensation algorithm to fulfill its duty. Careful analysis must always be performed with respect to the thermostat case design as well as the expected heat to be generated in the thermostat during varying current loads. This analysis can help ensure design robustness, along with temperature testing in the expected range to which the device will be subjected.

Several considerations are taken into account for this particular design:

- Standard thermostat set temperature
- PCB design for component heat localization
- Poly plane heat capacity to minimize influence on surface temperature sensor 1
- HVAC cycle turnon temperature threshold
- HVAC system cooling cycle time

These considerations apply to most temperature compensation designs in some way, but the designer must decide the particular considerations to take into account for a specific design.

TIDUDO1 翻訳版 — 最新の英語版資料 http://www-s.ti.com/sc/techlit/TIDUDO1
Copyright © 2018, Texas Instruments Incorporated

2.3 Highlighted Products

2.3.1 CC3220 LaunchPad

The CC3220x device is part of the SimpleLink™ microcontroller (MCU) platform, which consists of Wi-Fi®, *Bluetooth*® low energy, Sub-1 GHz, and host MCUs, all which share a common, easy-to-use development environment with a single core software development kit (SDK) and rich tool set. A one-time integration of the SimpleLink platform enables one to add any combination of the portfolio's devices into the design, allowing 100% code reuse when design requirements change. For more information, visit www.ti.com/simplelink.

Start an Internet-of-Things (IoT) design with a Wi-Fi CERTIFIED® single-chip MCU System on Chip (SoC) with built-in Wi-Fi connectivity. Created for IoT, the SimpleLink CC3220x device family from Texas Instruments is a single-chip solution, integrating two physically separated, on-chip MCUs.

- An application processor, the Arm® Cortex®-M4 MCU with a user-dedicated 256KB of RAM, and an optional 1MB of XIP flash
- A network processor MCU to run all Wi-Fi and Internet logical layers. This ROM-based subsystem includes an 802.11b/g/n radio, baseband, and MAC with a powerful crypto engine for fast, secure internet connections with 256-bit encryption.

The CC3220x wireless MCU family is part of the second generation of TI's Internet-on-a-chip™ family of solutions. This generation introduces new features and capabilities that further simplify the connectivity of things to the Internet. The new capabilities including the following:

- IPv6
- Enhanced Wi-Fi provisioning
- Enhanced power consumption
- Enhanced file system security (supported only by the CC3220S and CC3220SF devices)
- Wi-Fi AP connection with up to four stations
- More concurrently opened BSD sockets; up to 16 BSD sockets, of which 6 are secure
- HTTPS support
- RESTful API support
- Asymmetric keys crypto library

The CC3220x wireless MCU family supports the following modes: station, AP, and Wi-Fi Direct®. The device also supports WPA2 personal and enterprise security. This subsystem includes embedded TCP/IP and TLS/SSL stacks, HTTP server, and multiple Internet protocols. The device supports a variety of Wi-Fi provisioning methods including HTTP based on AP mode, SmartConfig™ technology, and WPS2.0.

The power-management subsystem includes integrated DC/DC converters that support a wide range of supply voltages. This subsystem enables low-power consumption modes for extended battery life, such as low-power deep sleep, hibernate with RTC (consuming only 4.5 µA), and shutdown mode (consuming only 1 µA).

The device includes a wide variety of peripherals, including a fast parallel camera interface, I2S, SD, UART, SPI, I^{2}C, and four-channel nanopower sensor monitor.

The SimpleLink CC3220x device family comes in three different device variants: CC3220R, CC3220S, and CC3220SF.

TIDUDO1 翻訳版 — 最新の英語版資料 http://www-s.ti.com/sc/techlit/TIDUDO1
Copyright © 2018, Texas Instruments Incorporated

The CC3220R and CC3220S devices include 256KB of application-dedicated embedded RAM for code and data, ROM with external serial flash bootloader, and peripheral drivers.

The CC3220SF device includes application-dedicated 1MB of XIP flash and 256KB of RAM for code and data, ROM with external serial flash bootloader, and peripheral drivers. The CC3220S and CC3220SF device options have additional security features, such as encrypted and authenticated file systems, user IP encryption and authentication, secured boot (authentication and integrity validation of the application image at flash and boot time), and more.

The CC3220x device family is a complete platform solution including software, sample applications, tools, user and programming guides, reference designs, and the E2E online community. The device family is also part of the SimpleLink MCU portfolio and supports the SimpleLink developers ecosystem.

- CC3220x SimpleLink Wi-Fi Wireless MCU SoC is a single chip with two separate execution environments: a user application dedicated Arm Cortex-M4 MCU and a network processor MCU to run all Wi-Fi and Internet logical layers
- Chip-Level, Wi-Fi Alliance certified
- Applications MCU subsystem:
  - Arm Cortex-M4 Core at 80 MHz
  - Embedded memory:
    - The CC3220R and CC3220S variants include 256KB of RAM
    - The CC3220SF variant is a flash-based wireless MCU with integrated 1MB of flash and 256KB of RAM
    - External serial flash
  - McASP supports two I2S channels
  - SD
  - SPI
  - I^2C
  - UART
  - 8-bit parallel camera
  - Four general-purpose timers with 16-bit PWM mode
  - Watchdog timer
  - Four-channel, 12-bit, nanopower sensor monitors
  - Up to 27 GPIO pins
  - Debug interfaces: JTAG, cJTAG, SWD
- Wi-Fi network processor (NWP) subsystem:
  - Wi-Fi Internet-on-a-chip dedicated Arm MCU completely offloads Wi-Fi and Internet protocols from the application MCU
  - Wi-Fi modes:
    - 802.11b/g/n station
    - 802.11b/g access point (AP) supports up to four stations
    - Wi-Fi direct client and group owner
  - WPA2 personal and enterprise security: WEP, WPA/WPA2 PSK, WPA2 Enterprise (802.1x)

Copyright © 2018, Texas Instruments Incorporated

- IPv4 and IPv6 TCP/IP Stack
- Industry-standard BSD socket application programming interfaces (APIs)
  - 16 simultaneous TCP or UDP sockets
  - 6 simultaneous TLS and SSL sockets
- IP addressing: Static IP, LLA, DHCPv4, DHCPv6 With DAD
- SimpleLink connection manager for autonomous and fast Wi-Fi connections
- Flexible Wi-Fi provisioning with SmartConfig technology, AP mode, and WPS2 options
- RESTful API support using the internal HTTP server
- Embedded network applications running on dedicated network processor
- Wide set of security features:
  - Hardware features:
    - Separate execution environments
    - Device identity
    - Hardware crypto engine for advanced fast security, including: AES, DES, 3DES, SHA2, MD5, CRC, and Checksum
    - Initial secure programming:
      - Debug security
      - JTAG and debug ports are locked
    - Personal and enterprise Wi-Fi security
    - Secure sockets (SSLv3, TLS1.0/1.1/TLS1.2)
  - Networking security:
    - Personal and enterprise Wi-Fi security
    - Secure sockets (SSLv3, TLS1.0, TLS1.1, TLS1.2)
    - HTTPS server
    - Trusted root-certificate catalog
    - TI root-of-trust public key
  - SW IP protection:
    - Secure key storage
    - File system security
    - Software tamper detection
    - Cloning protection
    - Secure boot: Validate the integrity and authenticity of the runtime binary during boot
- Embedded network applications running on the dedicated network processor:
  - HTTP/HTTPS web server with dynamic user callbacks
  - mDNS, DNS-SD, DHCP server
  - Ping
- Recovery mechanism can recover to factory defaults or to a complete factory image
- Wi-Fi TX power:

Copyright © 2018, Texas Instruments Incorporated

    - 18.0 dBm at 1 DSSS
    - 14.5 dBm at 54 OFDM
  - Wi-Fi RX sensitivity:
    - –96 dBm at 1 DSSS
    - –74.5 dBm at 54 OFDM
  - Application throughput:
    - UDP: 16 Mbps
    - TCP: 13 Mbps
- Power-management subsystem:
  - Integrated DC/DC converters support a wide range of supply voltage:
    - VBAT wide-voltage mode: 2.1 V to 3.6 V
    - VIO is always tied with VBAT
    - Preregulated 1.85-V mode
  - Advanced low-power modes:
    - Shutdown: 1 µA
    - Hibernate: 4.5 µA
    - Low-power deep sleep (LPDS): 135 µA (measured on CC3220R, CC3220S, and CC3220SF with 256-KB RAM retention)
    - RX traffic (MCU active): 59 mA (measured on CC3220R and CC3220S; CC3220SF consumes an additional 10 mA) at 54 OFDM
    - TX traffic (MCU active): 223 mA (measured on CC3220R and CC3220S; CC3220SF consumes an additional 15 mA) at 54 OFDM, maximum power
    - Idle connected (MCU in LPDS): 710 µA (measured on CC3220R and CC3220S with 256-KB RAM retention) at DTIM = 1
- Clock source:
  - 40.0-MHz crystal with internal oscillator
  - 32.768-kHz crystal or external RTC
- RGK package:
  - 64-pin, 9-mm × 9-mm very thin quad flat nonleaded (VQFN) package, 0.5-mm pitch
- Operating temperature:
  - Ambient temperature range: –40°C to +85°C
- Device supports SimpleLink developers ecosystem

Copyright © 2018, Texas Instruments Incorporated

2.3.2 TMP235

The TMP23x devices are a family of precision CMOS integrated-circuit linear analog temperature sensors with an output voltage proportional to temperature, making the series suitable for multiple analog temperature sensing applications. These temperature sensors are more accurate than similar pin-compatible devices on the market, featuring accuracy from 0°C to 70°C of ±1°C and ±2°C. The increased accuracy makes this series suitable for many analog temperature sensing applications. The TMP235 device provides a positive slope output of 10 mV/°C over the full –40°C to +150°C temperature range and a 2.3-V to 5.5-V supply range. The higher gain TMP236 sensor provides a positive slope output of 19.5 mV/°C from –10°C to +150°C and a 3.1-V to 5.5-V supply range.

The 9-µA typical quiescent current and 800-µs typical power-on time enable effective power-cycling architectures to minimize power consumption for battery-powered devices. A class-AB output driver provides a strong 500-µA maximum output to drive capacitive loads up to 1000 pF and is well-suited to directly interface to analog-to-digital converter sample and hold inputs. With excellent accuracy and a strong linear output driver, the TMP23x analog output temperature sensors are excellent, cost-effective alternatives to passive thermistors.

- Cost-effective alternative to thermistors
- Wide temperature measurement range: –40°C to +150°C
- Available in accuracy level variants:
  - ±0.5°C (typical)
  - ±1°C (typical)
- Positive slope sensor gain, offset (typical):
  - 10 mV/°C, 500 mV at 0°C
- Wide operating supply voltage range:
  - 2.3 V to 5.5 V
- Short-circuit protected output
- Low power: 9 µA (typical)
- Strong output for driving up to 1000-pF load
- Available package options:
  - 5-pin SC70 (DCK) surface mount
  - 3-pin SOT-23 (DBZ) surface mount

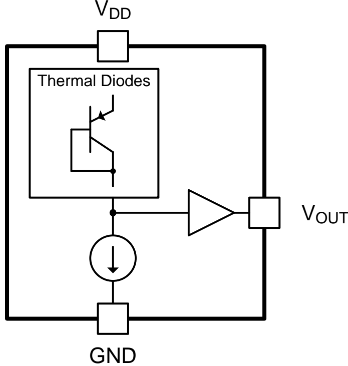

図 2. Functional Block Diagram of TMP235

Copyright © 2018, Texas Instruments Incorporated

2.3.3 INA230

The INA230 is a current-shunt and power monitor with an I^2C interface that features 16 programmable addresses. The INA230 monitors both shunt voltage drops and bus supply voltage. Programmable calibration value, conversion times, and averaging, combined with an internal multiplier, enable direct readouts of current in amperes and power in watts.

The INA230 senses current on buses that vary from 0 V to 28 V, with the device powered from a single 2.7-V to 5.5-V supply, drawing 330 μA (typical) of supply current. The INA230 is specified over the operating temperature range of –40°C to +125°C.

- Bus voltage sensing: 0 V to 28 V
- High- or low-side sensing
- Current, voltage, and power reporting
- High accuracy:
  - 0.5% gain error (maximum)
  - 50-μV offset (maximum)
- Configurable averaging options
- Programmable alert threshold
- Power supply operation: 2.7 V to 5.5 V
- Package: 3-mm × 3-mm, 16-pin QFN

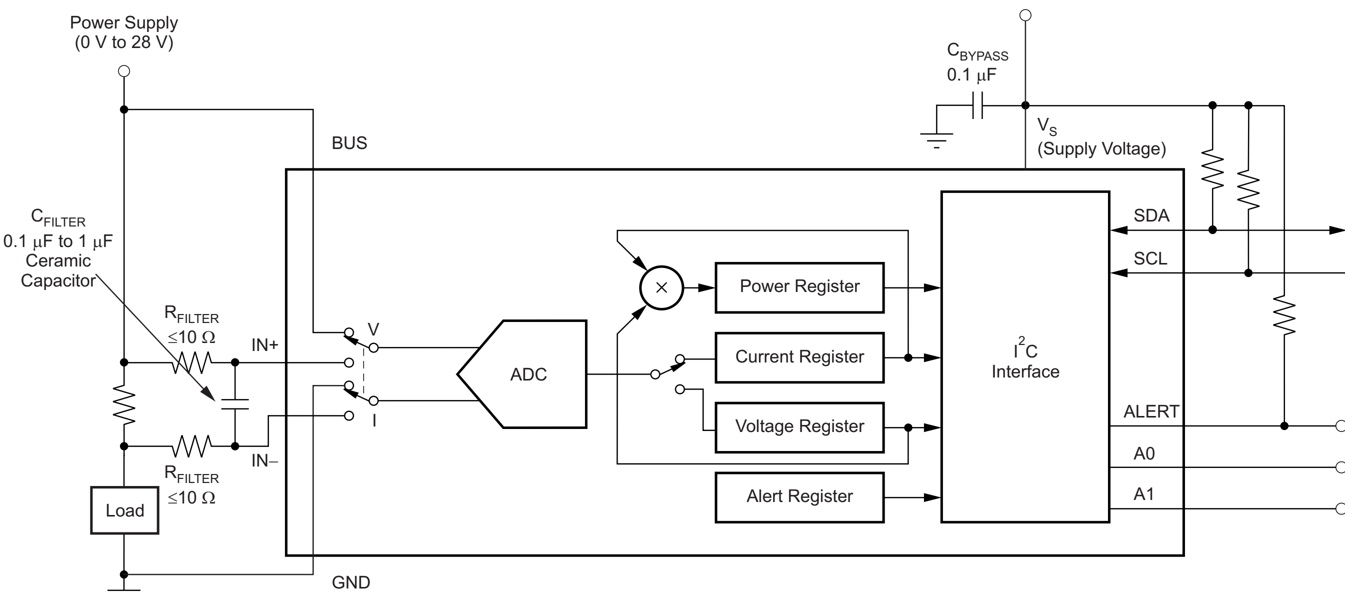

図 3. INA230 With Input Filtering

TIDUDO1 翻訳版 — 最新の英語版資料 http://www-s.ti.com/sc/techlit/TIDUDO1
Copyright © 2018, Texas Instruments Incorporated

2.3.4 ADS7142

The ADS7142 autonomously monitors signals while maximizing system power, reliability, and performance. The device implements event-triggered interrupts per channel using a digital windowed comparator with programmable high and low thresholds, hysteresis, and event counter. The device includes a dual-channel analog multiplexer in front of a successive approximation register analog-to-digital converter (SAR nanopower sensor monitor) followed by an internal data buffer for converting and capturing data from sensors.

The ADS7142 is available in 10-pin QFN package and consumes only 900 nW of power. The small form-factor and low power consumption make this device suitable for space-constrained and/or battery-powered applications.

- Standalone, nanopower sensor monitor for cost-sensitive designs
- Small package size: 1.5 mm × 2 mm
- Efficient host sleep and wake-up:
  - Autonomous monitoring at 900 nW
  - Windowed comparator for event-triggered host wake-up
  - Data buffering during host sleep
- Independent sensor configuration and calibration:
  - Dual-channel, pseudo-differential, or ground-sense input configuration
  - Programmable thresholds for calibration
  - Internal calibration improves offset and drift
- False trigger prevention:
  - Programmable thresholds per channel
  - Programmable hysteresis for noise immunity
  - Event counter for transient rejection
- Deep data analysis:
  - Data buffer for fault diagnostics
  - High precision mode for 16-bit accuracy
  - One-shot mode for fast data capture
- I²C interface:
  - Compatible from 1.65 V to 3.6 V
  - Eight configurable addresses
  - Up to 3.4 MHz (high speed)
- Wide operating range:
  - Analog supply: 1.65 V to 3.6 V
  - Temperature range: –40°C to +125°C

Copyright © 2018, Texas Instruments Incorporated

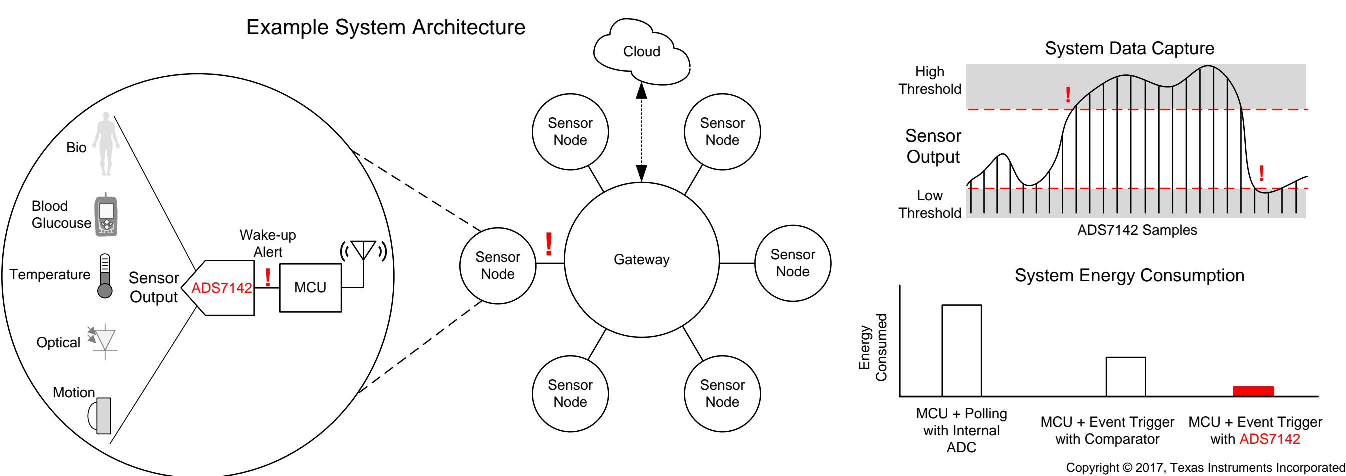

図 4. Example System Architecture

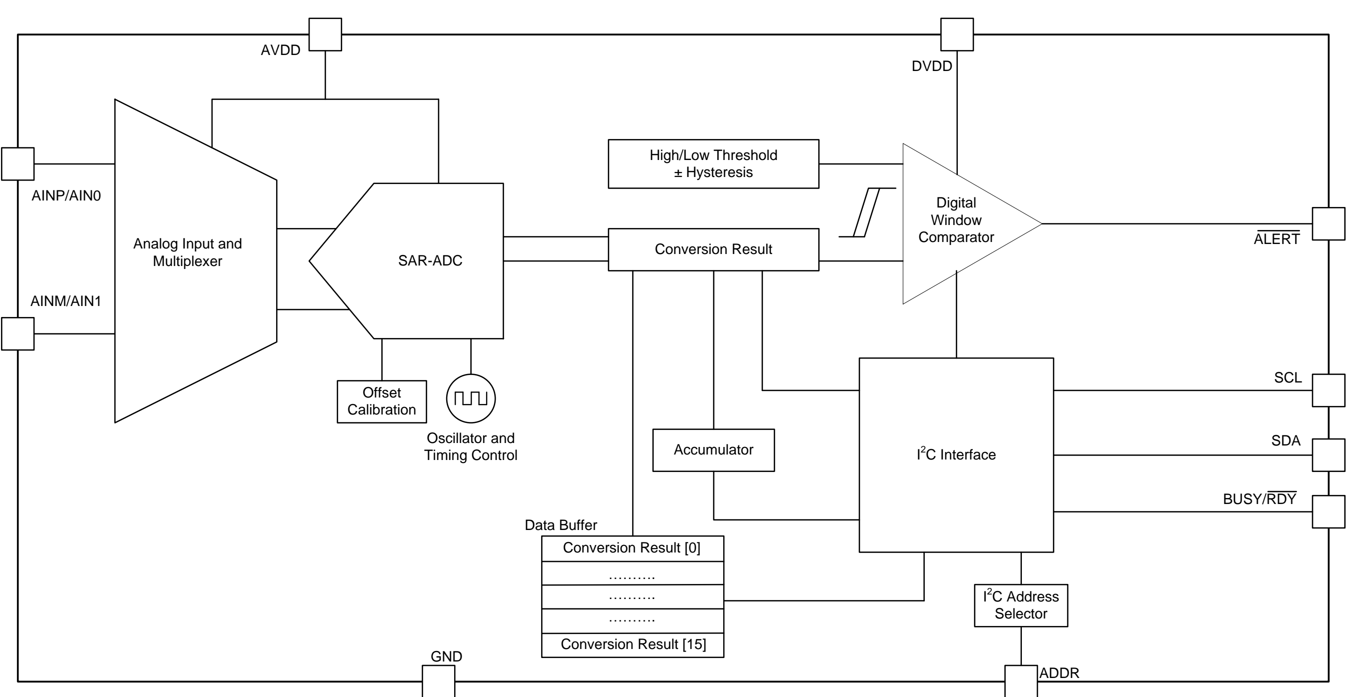

図 5. Functional Block Diagram of ADS7142

TIDUDO1 翻訳版 — 最新の英語版資料 http://www-s.ti.com/sc/techlit/TIDUDO1
Copyright © 2018, Texas Instruments Incorporated

2.3.5 LMT84

The LMT84 is a precision CMOS temperature sensor with ±0.4°C typical accuracy (±2.7°C maximum) and a linear analog output voltage that is inversely proportional to temperature. The 1.5-V supply voltage operation, 5.4-µA quiescent current, and 0.7-ms power-on time enable effective power-cycling architectures to minimize power consumption for battery-powered applications such as drones and sensor nodes. The LMT84LPG through-hole TO-92S package fast thermal time constant supports off-board time-temperature sensitive applications such as smoke and heat detectors. The accuracy over the wide operating range and other features make the LMT84 an excellent alternative to thermistors.

- LMT84LPG (TO-92S package) has a fast thermal time constant, 10-s typical (1.2 m/s airflow)
- Very accurate: ±0.4°C typical
- Low 1.5-V operation
- Average sensor gain: –5.5 mV/°C
- Low 5.4-µA quiescent current
- Wide temperature range: –50°C to +150°C
- Output is short-circuit protected
- Push-pull output with ±50-µA drive capability
- Footprint compatible with the industry-standard LM20/LM19 and LM35 temperature sensors
- Cost-effective alternative to thermistors

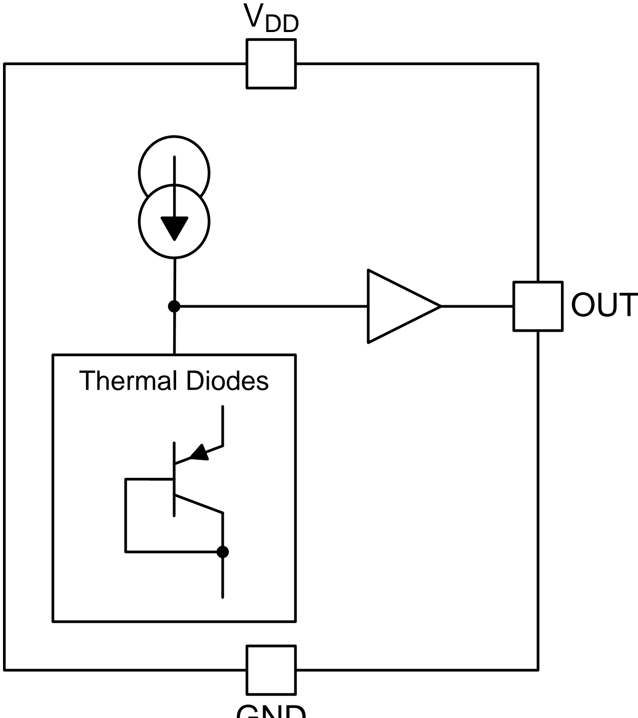

図 6. Functional Block Diagram of LMT84

TIDUDO1 翻訳版 — 最新の英語版資料 http://www-s.ti.com/sc/techlit/TIDUDO1
Copyright © 2018, Texas Instruments Incorporated

2.4 System Design Theory

2.4.1 Design Theory of Simulated Heat Load

To develop a solution to offset heat generated from internal components with respect to sensing the ambient room temperature, it is necessary to develop an accurate model of the heat generated inside the thermostat. In this particular design, a low-values power resistor is used in conjunction with an isolated DC voltage source to vary the heat load seen throughout the system as a whole.

To develop the necessary heat load, an estimated power consumption value is required for a typical household thermostat. After some preliminary statistical analysis, the average power consumption over a month is slightly less than 1 kW for smart thermostats. For design robustness and calculation simplicity, the power consumption is rounded to 1 kW. Using this value, the power consumption can be defined by 式 1:

$$P = \frac{1\,\text{kWh}}{\text{Month}} \times \frac{1\,\text{Month}}{30\text{ days}} \times \frac{1\text{ day}}{24\text{ hrs}} = 1.39\left(\frac{\text{W}}{\text{hr}}\right) = 386\left(\frac{\mu\text{W}}{\text{s}}\right) \tag{1}$$

Another control element that must be accounted for is the ability to vary the heat dissipation inside the thermostat casing. This ability is required because the seemingly low power consumption shown in generates additional heat over longer durations of time due to the continuous power consumption and the heat capacity of the internal thermostat components. Accounting for the conduction through surfaces and convection from the surfaces to the air, this heat eventually raises the internal thermostat temperature to a higher value. For more details on these thermodynamics, see 2.4.4.

For testing purposes, the hourly rate of consumption is used, assuming a single heating or cooling cycle will take place in that time frame. Using the value calculated in 式 1, use 式 2 to find the remainder of the required parameter values:

$$P = \frac{V^2}{R} \tag{2}$$

Here, the voltage range is arbitrarily defined as 5 V at its maximum, yielding a voltage range of 0 V to 5 V. Plugging in the known variable values yields:

$$R = \frac{V^2}{P} = \frac{25}{1.39} = 17.99\ \Omega \tag{3}$$

Adding in a buffer range for testing, the heat generation resistor is selected to be 20 Ω. This resistor results in a maximum current load of 250 mA for the simulated heat load portion of the board.

Because the test traces is subject to higher currents during the heat load simulation, the trace current capacity needs to be accounted for in this reference design. The only trace to verify in this particular case is from the sense resistor to the heat load resistor. As previously mentioned, the maximum expected current for this system is approximately 250 mA. The required trace width is found with both the IPC2221 standard, section 6.2, and the known trace attributes extracted from the layout. First the area is obtained using 式 4:

$$A = \left(\frac{i_{Limit}}{k \times (\Delta T)^b}\right)^{\frac{1}{c}} \tag{4}$$

where:

- K = 0.048
- B = 0.44

TIDUDO1 翻訳版 — 最新の英語版資料 http://www-s.ti.com/sc/techlit/TIDUDO1
Copyright © 2018, Texas Instruments Incorporated

- C = 0.725
- ΔT is experimentally set at 0.039°C for minimal heat generation

Replacing the variables with their respective values defined in the IPC2221 standard for external layers yields an area of 69.76 mils^2. The width of the trace can now be calculated as:

$$\text{Width} = \frac{A}{\text{thickness}} = \frac{69.76\ \text{mils}^2}{1.4\ \text{mils}} = 49.83\ \text{mils} \tag{5}$$

From this information, the following parameters as shown in 表 2 are calculated:

表 2. Simulation Circuit Trace Characteristics

PARAMETER	VALUE
Trace resistance	95.2 µΩ
Voltage drop across trace	23.8 µV
Power loss through trace	5.95 µW

The trace resistance value is added to the overall test circuit resistance for optimum accuracy in predicting the temperature offset due to the localized heat generation.

2.4.2 Design Theory of Current and Power Sensing

A lead indication of additional heat dissipation within a thermostat is the current consumption value of the system from the main power supply. As the current increases, so does the temperature. This relationship can be expressed through Joule's law:

$$Q = I^2 \times R \times t \tag{6}$$

where:

- Q is heat energy
- I is current in Amps
- R is resistance in Ohms
- t is duration of current flow in seconds

Using an INA230 bidirectional current and power monitor, the overall current consumption of the test circuit can be accurately obtained and used in 式 6 to obtain the heat energy produced. From this value, the energy of the circuit can be estimated using 式 7:

$$Q = m \times c \times (T_2 - T_1) \tag{7}$$

where:

- m is the mass of trace material
- c is the specific heat capacity of material
- T_2 is some time value obtained after T_1

Rearranging 式 7 to solve for the new temperature value gives the following:

$$T_2 = \frac{Q}{m \times c} + T_1 \tag{8}$$

式 8 can be used in conjunction with the known resistance and current consumption to obtain the localized heat generation given off by the test circuit. To accurately measure this value, the circuit resistance must be extracted from the design. This process is detailed in the following subsections.

TIDUDO1 翻訳版 — 最新の英語版資料 http://www-s.ti.com/sc/techlit/TIDUDO1
Copyright © 2018, Texas Instruments Incorporated

2.4.2.1 Simulation Circuit Characterization

図 7 shows the resistance extraction simulation setup of this reference design. SIwave is used to extract trace data pertaining to the RLC values of the trace and power planes connected to the power resistor. This simulation ignores any resistance added from the jumper; this is only added for testing purposes and is not assumed to be in an end-equipment design. The vias and poly clearance sections shown in 図 7 are kept in the simulation to provide accuracy.

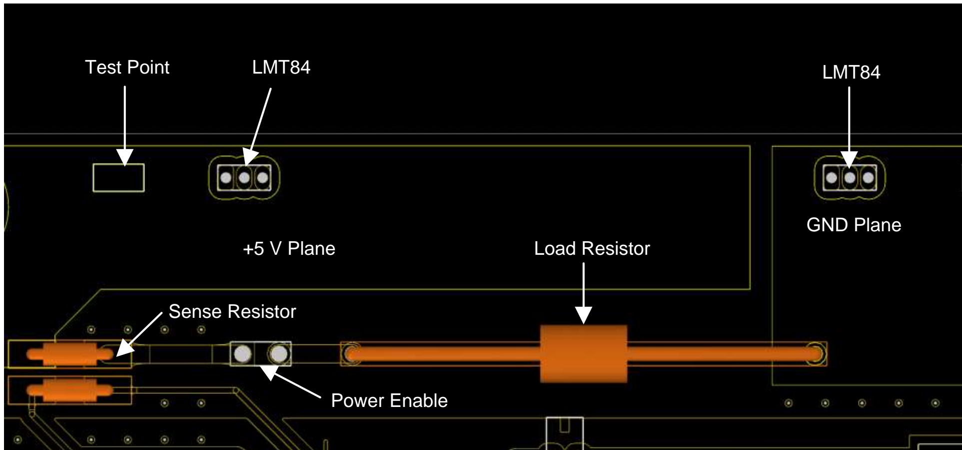

図 7. SIwave Simulation Circuit

Before the R-L-C values are extracted from the simulation layout, the layer stackup and vias are verified. This process is captured in 図 8 and 図 9. Ensure these parameters are as precise as possible compared to the actual board fabrication values to help optimize the effectiveness and accuracy of the simulation. For this simulation, copper is used for all trace and poly material and the dielectric layers are comprised of FR4 epoxy.

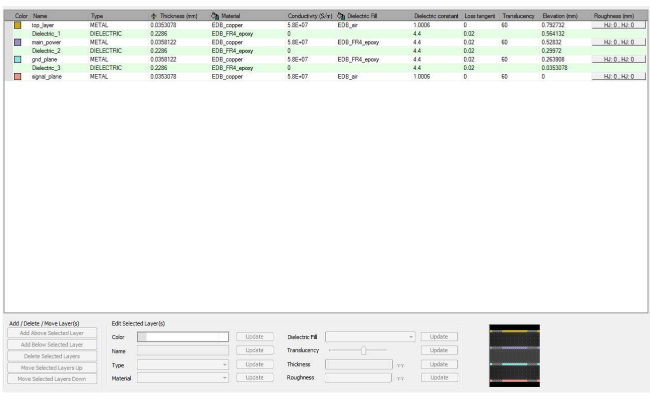

図 8. SIwave Layer Parameter Definition

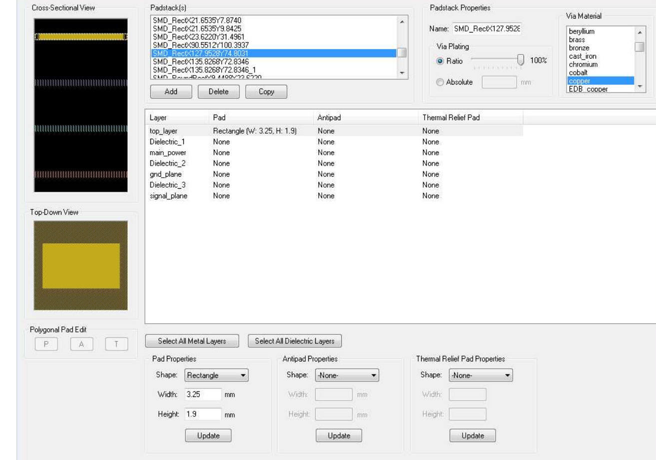

図 9. SIwave Padstack Parameter Definition

Copyright © 2018, Texas Instruments Incorporated

After these values are validated by the fabrication data, the R-L-C values are extracted from the layout. For the purpose of this design, only the resistance values are shown as they are the only variable whose value is considered in the calculations. 表 3 lists the dimensional values. As previously mentioned, the series jumper resistance is neglected in this particular design, but the additional resistance is extracted for the power monitoring sense resistor circuit, the connecting traces from the isolated DC input to the ground, and the poly planes used for the V+ and GND.

表 3. Simulation Circuit Trace Dimension Definition

TRACE, POLY, OR COMPONENT	MEASURED AREA	TRACE OR POLY THICKNESS
V_{IN_TEST} poly	577.23 mm^2	0.03556 mm
Trace 1	11.082 mm^2	0.03556 mm
Trace 2	6.4516 mm^2	0.03556 mm
V_{GND_TEST} poly	410.31 mm^2	0.03556 mm

For the parameters derived in 表 3, the value of the resistance of each path can be calculated using 式 9:

$$R = \rho \frac{\ell}{A} \quad (9)$$

where:

- ρ is the resistivity of the material
- ℓ is the length of the material with respect to the direction of current flow
- A is the cross-sectional area of the material

表 4 lists the calculated values.

表 4. Simulation Circuit Trace Resistance

TRACE, POLY, OR COMPONENT	RESISTANCE VALUE
V_{IN_TEST} poly	294.62 mΩ
Current sense resistor	50 mΩ
Trace 1	92 mΩ
Trace 2	88 mΩ
Heat simulation resistor	20 Ω
V_{GND_TEST} poly	146 mΩ

Once these values are extracted, a DC IR drop simulation is also done to show the current density and the voltage distribution through the board. This simulation aids in locating the hot points of the board before manufacturing. 図 10 shows the results. The current density is shown to be much more biased towards the supply plane, indicating a higher voltage bias in this area as well. This result shows a preliminary prediction of the heat distribution from the test circuit traces, neglecting the discrete components, which are accounted for later.

The total heat dissipation from the testing plane is determined to be 9.41E-10 W. This result indicates that there is good isolated thermal energy dissipation, which will have a minimal effect on the overall results with respect to the localized heat offset correction. This correction is important because this data can be used as a precursor for the heat dissipated through the internal layers of the board to the back, where the isolated temperature sensor is placed for ambient temperature readings. For more details on the these sensors, see 2.4.3.

TIDUDO1 翻訳版 — 最新の英語版資料 http://www-s.ti.com/sc/techlit/TIDUDO1
Copyright © 2018, Texas Instruments Incorporated

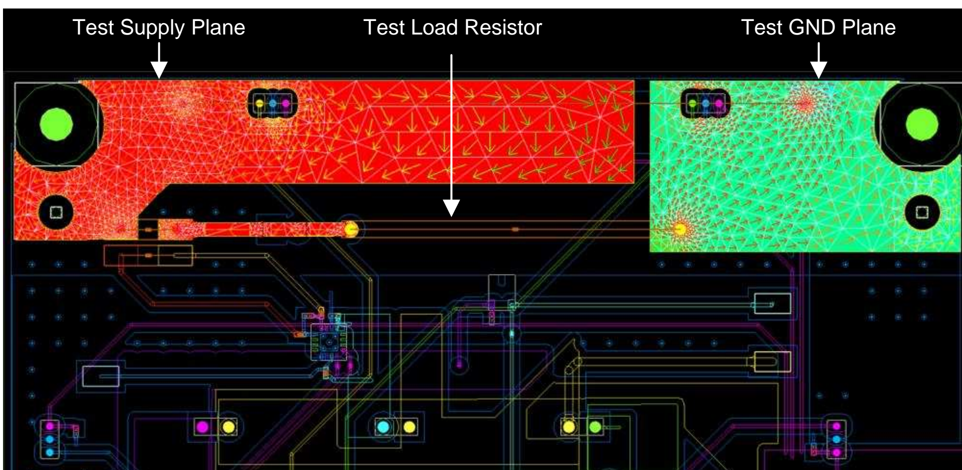

図 10. SIwave DC-IR Simulation Results

This simulation represents the ideal environmental conditions and does not take into account the temperature variations seen in a typical household. These additional conditions can affect the trace resistance properties of the board, leading to slight variations from the results shown in 図 10 and 表 4. For this reason, a preliminary test board is prepared to analyze the overall resistance variation over household temperature extremes (32°F to 100°F). 表 5 and 図 11 show the resulting resistance of the complete test circuit over these temperatures and a typical household temperature.

表 5. Extracted Resistance Values Over Temperature

SET TEMPERATURE	MEASURED RESISTANCE	ΔR
32°F	20.034 Ω	34 mΩ
100°F	20.010 Ω	10 mΩ
72°F	20.024 Ω	24 mΩ

The measured resistance is shown to change rapidly once the temperature is adjusted before coming to a steady state resistance value. Analyzing the results further shows the steady state resistance is slightly different for each of the temperatures tested. Point A is the point at which the temperature settles after a temperature swing from 100°F to 32°F for maximum dynamic change. The resistance eventually settles back to the 32°F steady state resistance obtained previously in the plot.

TIDUDO1 翻訳版 — 最新の英語版資料 http://www-s.ti.com/sc/techlit/TIDUDO1
Copyright © 2018, Texas Instruments Incorporated

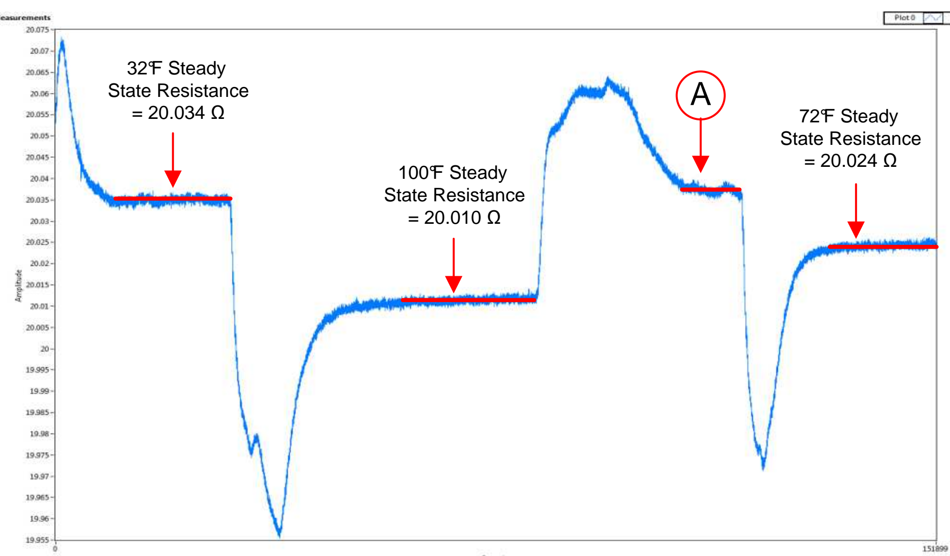

図 11. Resistance Variation Over Temperature

The transient resistance values are neglected in this reference design due to the testing conditions. This rapid change is due to the small 1-ft^2 thermal chamber and the ability to rapidly change temperature. This change is much more linear in a typical household environment.

Using these values, the temperature coefficient of resistance (TCR) can be calculated. Although the TCR in this particular temperature range is insignificant, the value is calculated for the purpose of demonstrating the analysis process. The TCR is determined using 式 10:

$$TCR = \frac{R_2 - R_1}{R_1 \times (T_2 - T_1)} 10^{-6} \tag{10}$$

Adding in the known variable values previously extracted, the TCR value is calculated to be:

$$TCR = \frac{20.01 - 20.034}{20.034 \times (37.7778 - 0)} 10^{-6} = \boxed{\left(-3.17 \times 10^{-11}\right) \frac{ppm}{°C}}$$

This variation in temperature can be taken into account for more accurate sensing based on the sensed internal temperature of the system and in systems where the temperature dynamics will be more significant. Using the resistance values previously calculated, the temperature increase can be calculated using 式 6 and 式 7. Adding in the known variable values and assuming a steady state ambient air temperature of 72°F, a specific heat value of 0.385 J/g°C, and a total trace mass of 316.15 mg yields:

$$Q = (0.250\,A)^2 \times 20.024\,\Omega \times 1\,s = 1.2515\ Joules \tag{11}$$

$$T_2 = \frac{1.2515\,J \times °C}{0.31615\,g \times \frac{0.385\,J}{g}} + 22.22°C = 32.50°C \tag{12}$$

The test trace generates enough heat energy in 1 second to increase its temperature by 10°C, or roughly 18°F. However, this equation does not take into account the surrounding material that also absorbs the heat energy given off by this test circuit. This heat energy eventually increases the temperature of components and air surrounding the test circuit through conduction and convection, which causes the ambient temperature offset in thermostats. For this reason, the test circuit is used in addition to the calculated results for accurate modeling. This heat energy dissipation is explored further in 2.4.3.

Copyright © 2018, Texas Instruments Incorporated

This test circuit configuration gives the designer the ability to work with many voltage steps to produce the target amount of heat generated by their own system. The current here is related to the voltage input to the test circuit, so finding the heat energy for a smaller load can be done by simply replacing the current value with the new values and recalculating the values.

2.4.2.1.1 Setting up INA230 Registers

To measure the current of the system to relate to the previously derived formulas, the INA230 device is used in conjunction with a four-port, 50-mΩ resistor to obtain the current and power consumption of the test load. The LVK resistor has four terminals, better known as a "Kelvin" configuration. This configuration enables current to be applied through two terminals and a sensing voltage to be measured across the other two terminals, eliminating the resistance and temperature coefficient of the terminals for a more accurate current measurement. Isolating the voltage and current terminals facilitates a very accurate current measurement. The following describes the register setup used for this particular design.

The calibration register is calculated based on 式 13. 式 13 includes the term Current_LSB, which is the programmed value for the LSB for the current register. This variable is the value used to convert the value in the current register to the actual current in amps. The highest resolution for the current register can be obtained by using the smallest allowable Current_LSB based on the maximum expected current, as shown in 式 14. While this value yields the highest resolution, it is common to select a value for the Current_LSB to the nearest round number above this value to simplify the conversion of the current register and power register to amps and watts, respectively. R_{SHUNT} is the value of the external shunt used to develop the differential voltage across the input pins. The 0.00512 value in 式 13 is an internal fixed value used to ensure scaling is maintained properly.

$$CAL = \frac{0.00512}{Current_LSB \times R_{SHUNT}} \tag{13}$$

$$Current_LSB = \frac{Maximum\ Expected\ Current}{2^{15}} \tag{14}$$

After the calibration register has been programmed, the current register and power register are updated accordingly based on the corresponding shunt voltage and bus voltage measurements. Until the calibration register is programmed, the current and power registers remain at zero.

In this application, a nominal 250-mA load creates a differential voltage across a 50-mΩ shunt resistor. The bus voltage for the INA230 is measured at the external BUS input pin; in this case, BUS is connected to the IN– pin to measure the voltage level delivered to the load.

Assuming a maximum expected current of 250 mA, Current_LSB is calculated to be 7.63 µA/bit using 式 14 with a shunt resistor of 50 mΩ, resulting in a calibration register value of 13422, or 346Eh. The current register (04h) is then calculated by multiplying the decimal value of the shunt voltage register contents by the decimal value of the calibration register and then dividing by 2048, as shown in 式 15.

$$Current = \frac{ShuntVoltage \times CalibrationRegister}{2048} \tag{15}$$

The LSB for the bus voltage register (02h) is a fixed 1.25 mV/bit. Note that the MSB of the bus voltage register is always zero because the BUS pin is only able to measure positive voltages. The power register (03h) can be calculated by multiplying the decimal value of the current register by the decimal value of the bus voltage register and then dividing by 20000, as defined in 式 16.

$$Power = \frac{Current \times BusVoltage}{20{,}000} \tag{16}$$

Copyright © 2018, Texas Instruments Incorporated

For more information on the programming of the INA230 device, see http://www.ti.com/product/INA230.

2.4.3 Design Theory of Surface Temperature Sensor Network

The temperature sensor network consists of two separate device combinations comprised of analog temperature sensors. The design also can be used with thermistors as well for system specific testing. The first set of temperature sensors consist of two TMP235 temperature sensors. These sensors provide low power consumption as well as a high accuracy at a low cost. These sensors are placed in two distinct locations of the board. One is placed locally to the heat load—in this particular case, the power resistor. The remaining temperature sensor is placed on the bottom side of the test board, and closer to the edge of the board.

This placement allows the designer to measure the temperature increase of the heat generating components in the thermostat during an HVAC cycle, as well as the temperature closest to the ambient condition due to its placement at the edge of the board away from any heat sources. This temperature can be determined through the use of thermal analysis of the worst case scenario, a 250-mA load in this case. 図 15 shows the thermal image of this reference design during a maximum load condition. Temperature sensor 1 is placed near the edge of the board on the bottom where there is relatively little influence by component heat on the temperature reading (see 図 12). Temperature sensor 2 is placed as close to the source as possible (see 図 14).

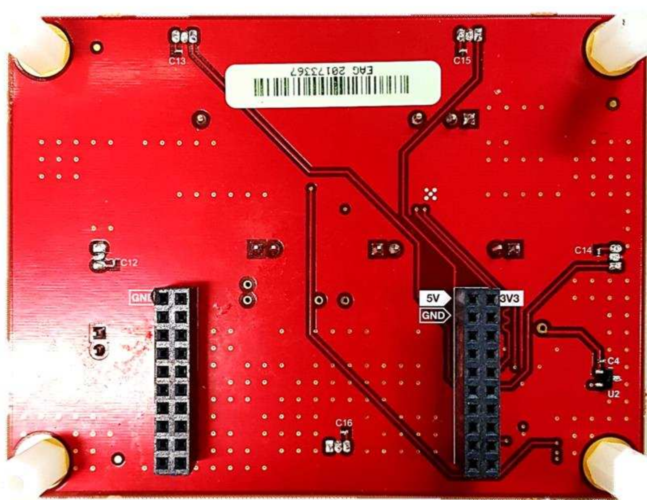

図 12. TMP235 Sensor 1 Location (Isolated)

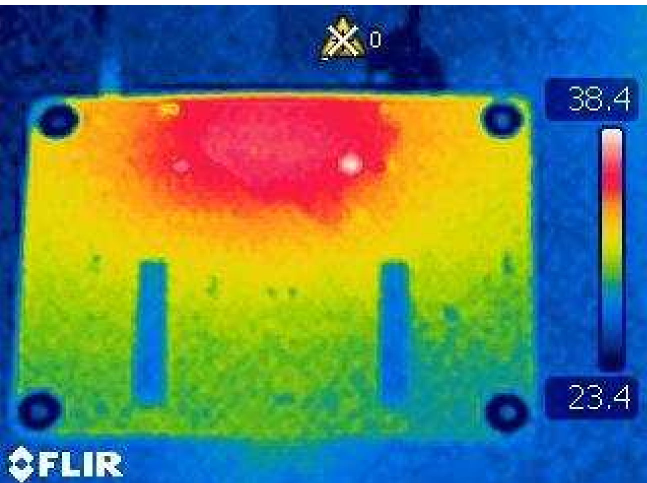

図 13. Bottom PCB Thermal Dissipation Analysis

Copyright © 2018, Texas Instruments Incorporated

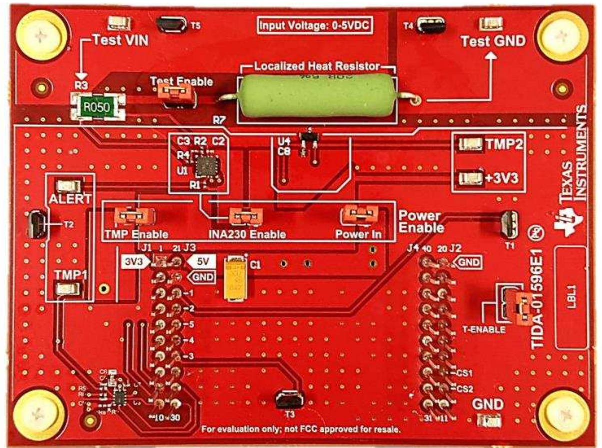

図 14. TMP235 Sensor 2 Location (Load)

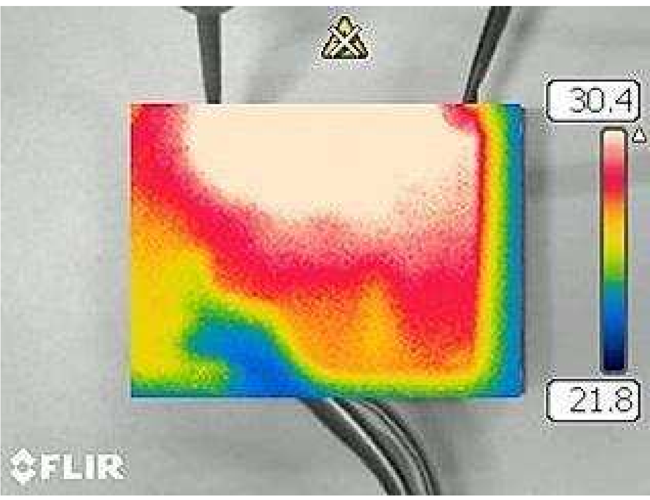

図 15. Top PCB Thermal Dissipation Analysis

This method is good for PCB boards with more heat generating parts placed on a single side of the PCB. For this case, ensure most of the heat dissipated throughout the PCB occurs mostly on the first few layers with little-to-no short-term influence on the bottom layer. This influence can be verified through both simulation and thermal image analysis.

2.4.4 Design Theory of Convective Temperature Sensing

Another set of temperature sensors is placed on the board for an alternative method. Five LMT84 analog temperature sensors are placed around the perimeter of the board. 図 16 shows the specific locations of each sensor. The placement for the sensors can be moved about the PCB based on specific design requirements. For this reference design, there are two temperature sensors placed closer to the heat load, near the edge of the board. Two more sensors are placed opposite of each other (T1 and T2), also on the edge of the board. Finally, T3 is placed in the middle of the board slightly inward from the bottom edge of the PCB.

For this particular set of sensors, the devices are slightly elevated from the surface of the PCB to measure the rise in air temperature between the circuitry and the interface to the ambient environment. This method enables the designer to analyze the convective heat transfer into the air of the internal cavity without necessarily needing the PCB board temperature.

The sensors are arranged to encompass the heat generation portion of the board. From this, the designer has many options on how to implement the temperature offset correction and can also be used to determine the influence on internal heat generation that a particular component, or cluster of components, has on the system as a whole. This method can be more challenging than the others due to the delay in temperature change due to ambient influence.

Copyright © 2018, Texas Instruments Incorporated

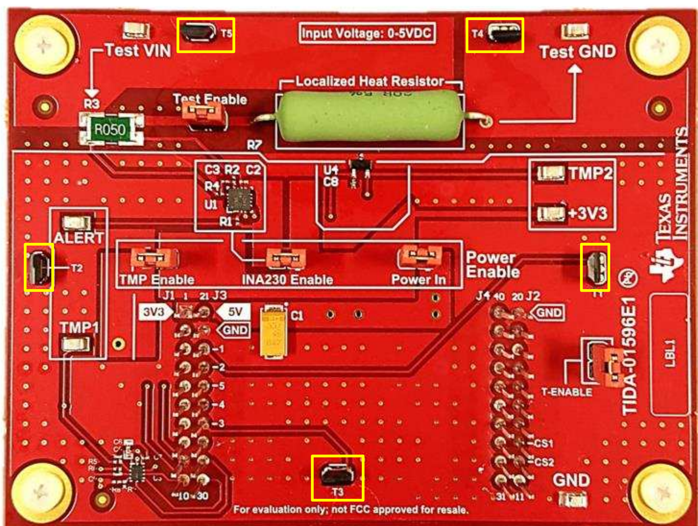

図 16. LMT84 PCB Locations for Convective Sensing

Copyright © 2018, Texas Instruments Incorporated

2.4.5 Design Theory of Thermodynamic Simulation Model

To predict or verify the behavior of the testing setup, the previously obtained values and parameters are used in conjunction with a MATLAB® thermal simulation. This simulation is used to predict the heat absorbed by the air in the thermostat case as well as the heat conducted through the thermostat case material. 図 17 shows the simulation layout, which is how the value obtained in 図 27 dissipated throughout the board and the surrounding elements.

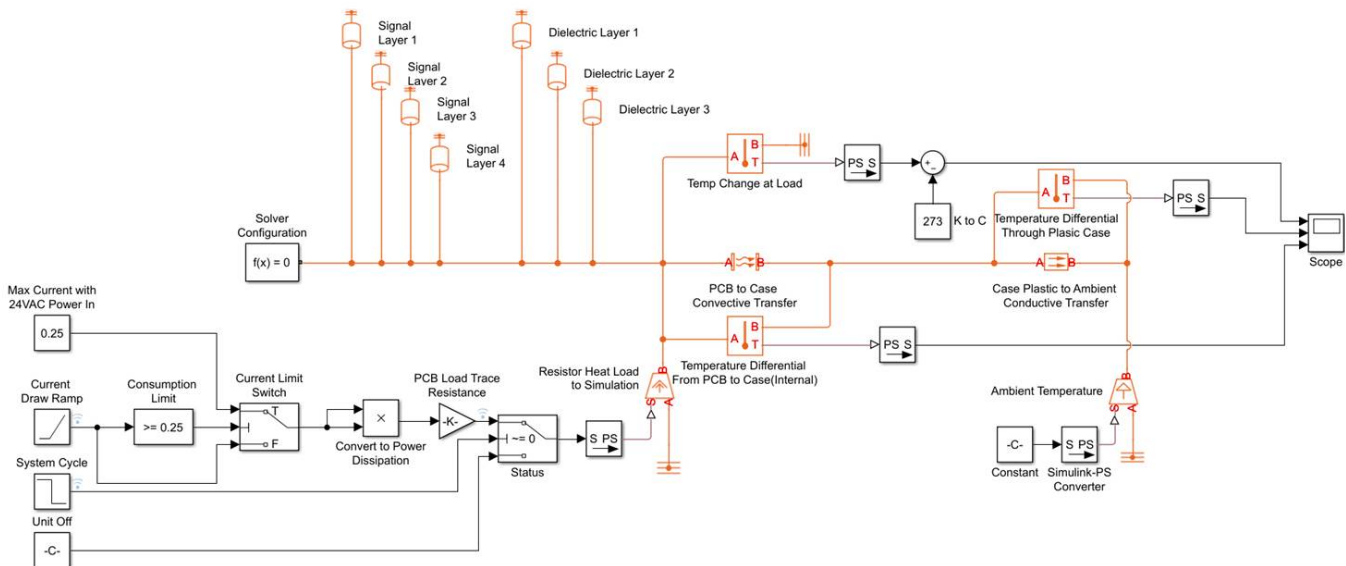

図 17. MATLAB Thermodynamic Simulation Schematic

Referencing 図 17, the MATLAB simulation is split into four main sections:

- namely the HVAC cycle behavior section
- the modeling of materials within the simulation with the ability to retain a particular amount of heat
- the thermodynamic modeling of both conductive as well as convective heat transfer

These simulation signals are output to a software-based scope to observe the behavior of the system under various loads.

TIDUDO1 翻訳版 — 最新の英語版資料 http://www-s.ti.com/sc/techlit/TIDUDO1
Copyright © 2018, Texas Instruments Incorporated

2.4.5.1 Thermostat Model

The first section of the simulation is the components that mimic the behavior of a typical household AC system. For this section, the current is set to a limit of 250 mA as determined in the previous sections. Because the current consumption of the system cannot be instantaneous, a ramp function is used to allow more flexibility and complexity in current consumption modeling. This ramp is based on a slope, not a final current value; for this reason, a current limit switch is placed in series with the current elements of this subsection to switch to a constant current value after reaching a certain point in the ramp cycle. If this is not placed in the simulation, the load current continues to increase indefinitely.

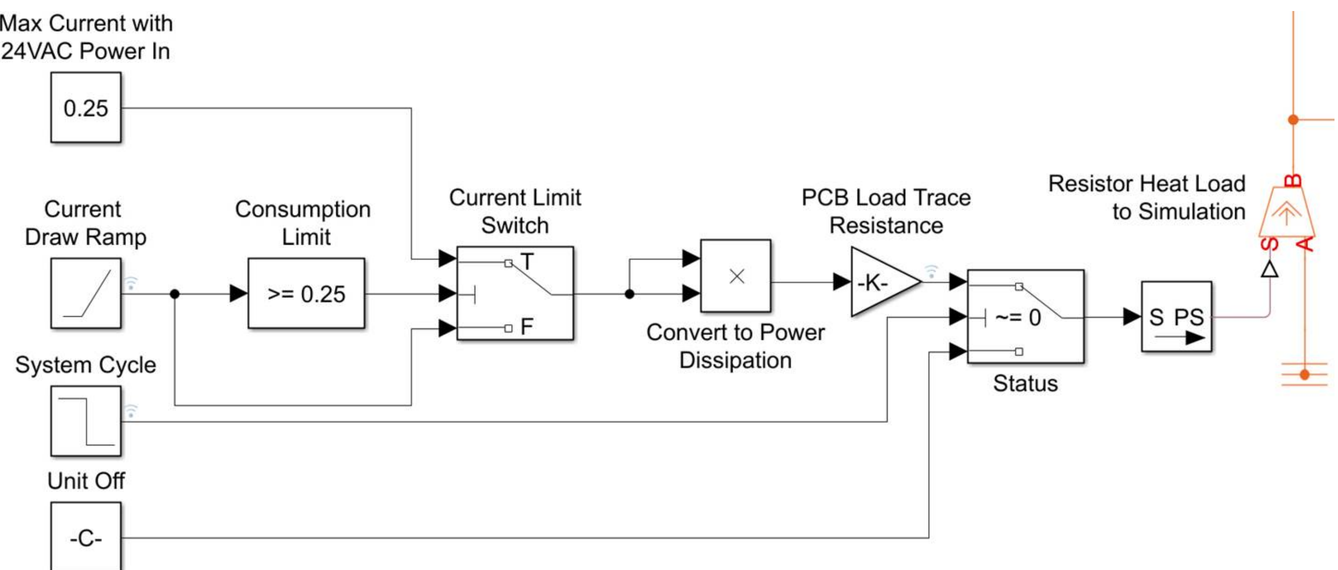

図 18. Simulation of Signal Chain of HVAC Thermostat Cycle

The system cycle waveform is a simple square wave that initiates the system cycle further down the system model signal chain. For the thermal output values, the units are defined in Celsius with respect to the remainder of the system. This is due to the requirement of some simulation blocks to have a Kelvin unit input temperature, and the direct relation between a differential in Kelvin, and the differential in Celsius.

The next part of the signal chain converts the previous elements into a power consumption value using the test trace resistance found earlier. Lastly, the signal is converted into a physical signal as per MATLAB requirements before introducing the heat generation model into the rest of the system.

Copyright © 2018, Texas Instruments Incorporated

2.4.5.2 Thermal Mass Model

The next part of the simulation involves defining the materials in the system that have the capability to store internal energy. This capability is defined by the materials specific heat capacity as well as the mass associated with each defined element.

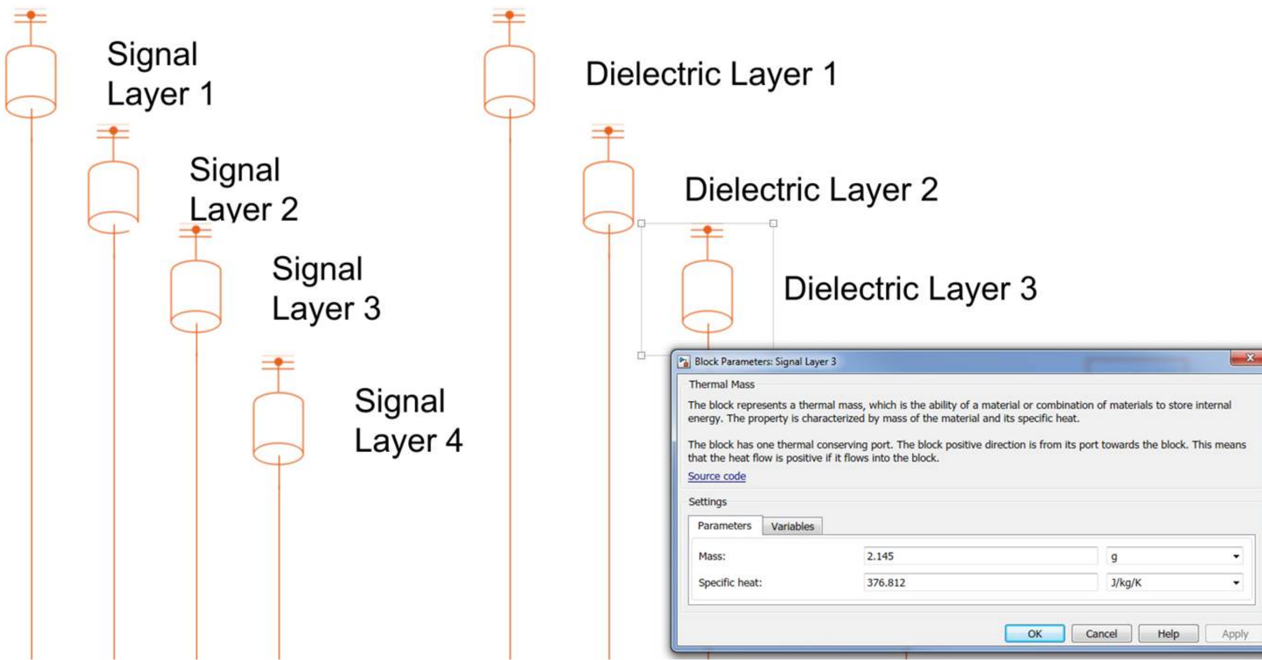

図 19. Simulation Definition of Thermal Mass

For this reference design, the main heat absorbing and retaining material is defined before the remainder of the thermodynamic energy transfer is introduced to the system. The values used for these elements are defined through the heat load capacity values specified in the manufacturer data sheet in addition to the dimensional values derived previously. 2.4.5.3 shows these parameters used for the MATLAB simulation.

表 6. Simulation System Parameter Definition

PARAMETER	MATERIAL	DIMENSIONS	MASS	SPECIFIC HEAT
Trace layers	Copper	3.7' × 2.9'	3.06 g	1300 J/kg/K
Dielectric layers	FR4 epoxy	3.7' × 2.9'	2.145 g	376.812 J/kg/K

TIDUDO1 翻訳版 — 最新の英語版資料 http://www-s.ti.com/sc/techlit/TIDUDO1
Copyright © 2018, Texas Instruments Incorporated

2.4.5.3 Energy Transfer Model

From this, the temperature dissipation from the test circuit to the internal cavity space air through convection is estimated along with the conduction through the PCB and the thermostat case. 表 7 shows the thermostat case parameters used to test this reference design. Accuracy in this design is crucial in developing and understanding the absorption of the heat energy and the thermal offset due to the heat load.

表 7. Energy Transfer Simulation Parameter Values

PARAMETER	HEAT TRANSFER COEFFICIENT OR THERMAL CONDUCTIVITY	MATERIAL	AREA
PCB to case convective transfer	10 W/(m² × K)	Air	10.36 in²
Case plastic to ambient conductive transfer	4.2803 W/(m × K)	Plastic + glass	36.204 in²

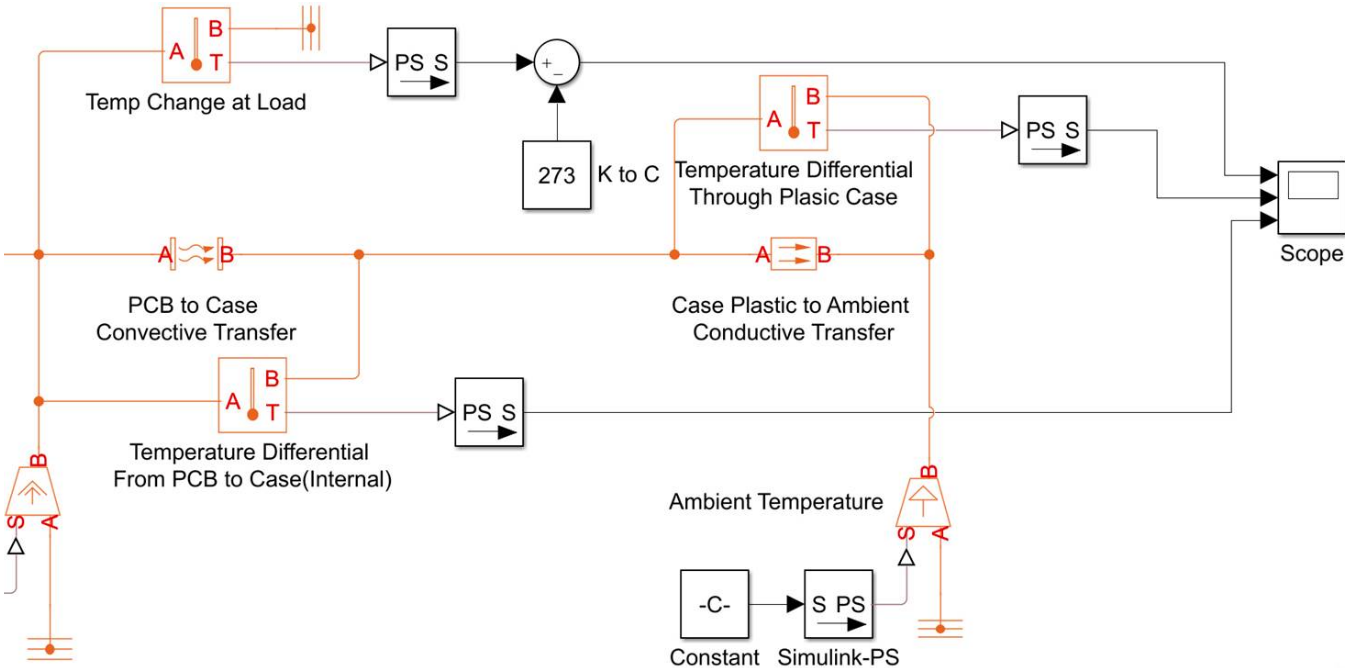

図 20. Model of Thermal Energy Dissipation

Copyright © 2018, Texas Instruments Incorporated

Once the simulation is set up with respect to the specific solver selection used, run the simulation to estimate the temperature differential between the load and the ambient temperature outside of the thermostat case. 図 21 and 図 22 show the results for the design board.

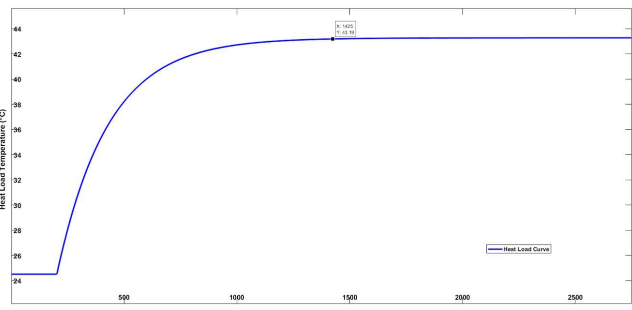

図 21. MATLAB Simulation of Estimated Load Temperature

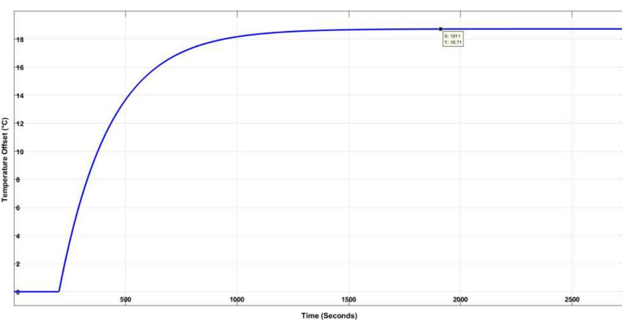

図 22. Estimated Temperature Offset From Load to Ambient in °C

This offset curve can be used to compare against the actual board offset and verify the accuracy of the simulation parameters, as shown in 図 45.

2.4.6 Development Theory of Temperature Offset Algorithm

As explained in 2.4.5.3, this reference design uses several different devices to measure the temperature offset due to localized component heat. There are numerous combinations of these devices that can be used to accurately measure this heat; this design guide highlights three main ways:

- Current monitor with temperature sensing (2.4.6.1)
- Two-sensor surface temperature sensing (2.4.6.2)
- Convective heat sensing method (2.4.6.3)

The following subsections outline the offset algorithm development process for these three methods. All three methods are characterized slightly offset from each other with respect to temperature range to allow each separate algorithm to run independently of the others for evaluation purposes. The user can modify this as desired.

One of the most unique features of this design is the autonomous sensor monitoring capabilities of the nano-powered ADS7142. This monitor allows the main MCU to shut down its own integrated ADC, lowering the power consumption of the system greatly by running the ADS7142 alone. This device only requires a restart once a certain user programmed threshold is reached. This feature is a must for systems that are power consumption and cost sensitive.

2.4.6.1 Current Monitor With Dual Temperature Sensing Method

This method combines the use of current monitoring with temperature sensing. Before developing the algorithm, preliminary test data is taken to characterize the behavior of the system with respect to these components. 図 24 shows the current and temperature relation of the test circuit in this reference design. The temperature rise is small until the current consumption reaches 50 mA. In this plot, the blue line represents the temperature of the internal cavity of the thermostat, and the red line shows the incremented load current applied to the test board. For this case, the temperature of the load in the case is acquired with a thermocouple placed directly in contact with the load resistor surface.

TIDUDO1 翻訳版 — 最新の英語版資料 http://www-s.ti.com/sc/techlit/TIDUDO1
Copyright © 2018, Texas Instruments Incorporated

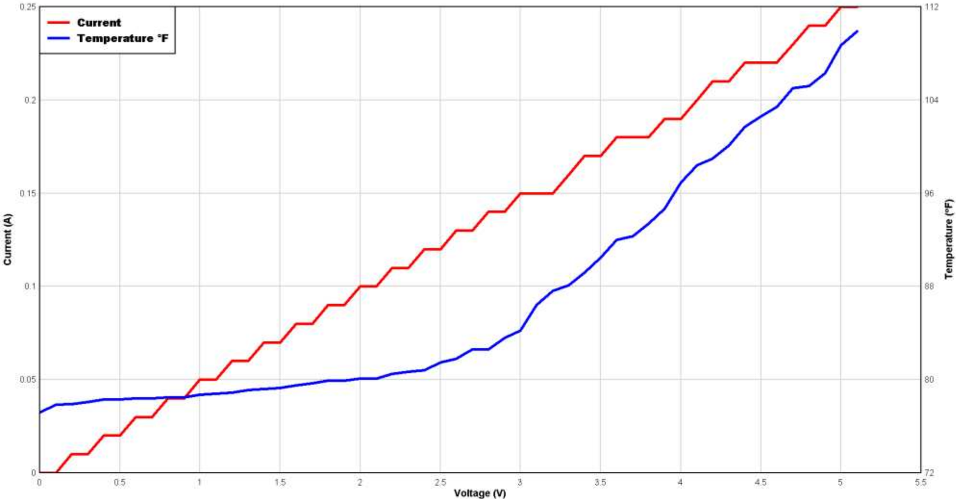

図 23. Current and Temperature Relation Based on Applied Voltage

This data can help determine a relationship to use in the firmware to correct the temperature offset. For this particular method, the current is increased through a voltage step size of 0.1 V. First, a relatively accurate equation of the curve is extracted through MATLAB. 図 24 shows the resulting poly-fit superimposed on the source curve as well as the respective mathematical relation between temperature and current at the load. The voltage curve is neglected in this curve fitting because it is only used for varying the current value at the load.

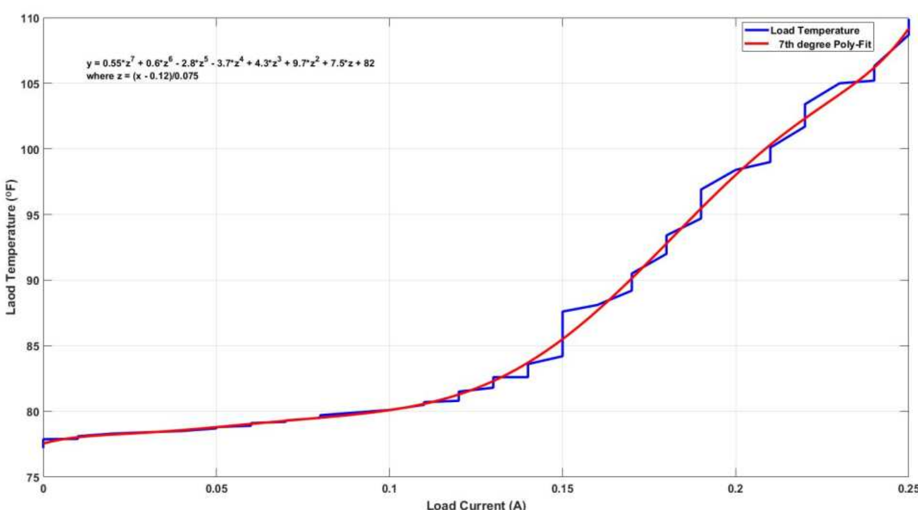

図 24. Test Circuit Load Current vs Sensed Load Surface Temperature

Copyright © 2018, Texas Instruments Incorporated

Using 式 17, the ambient temperature outside of the case can be estimated. First, the change in temperature over current is determined by a poly-fit curve based the differential between the two curves shown in 図 23, yielding:

$$y = 0.55z^7 + 0.6z^6 - 2.8z^5 - 3.7z^4 + 4.3z^3 + 9.7z^2 + 7.5z + 82 \quad (17)$$

where:

$$z = \frac{\text{Current} - 0.12}{0.075}$$

The temperature offset curve can be based on time interval implemented in firmware or a reference temperature; therefore, if needed, the correction factor can be determined for dynamic system cycles. For this reference design, the temperature value is referenced for an offset correction factor for simplicity. To use this method, the temperature differential over the distance between the load and sensor must be characterized.

From the test results in 図 25, the temperature differential between the nearest temperature sensor (TMP2) and the load at an initial temperature of 75°F is about 15°F. This value can be used as a reference temperature to which the temperature will eventually reach within 10 minutes, an assumed cycle of time that can be modified based on location and time of year. For example, it is assumed that for a 10-minute cycle at a 250-mA load, the temperature inside the thermostat case will reach upwards of 110°F.

Adding in the offset compensation with the temperature value of the TMP235, the offset value is obtained. The temperature change in this case is slightly faster due to the lower starting temperature, but is of no concern because the characteristic difference is what is needed from this data, independent of any time constraints.

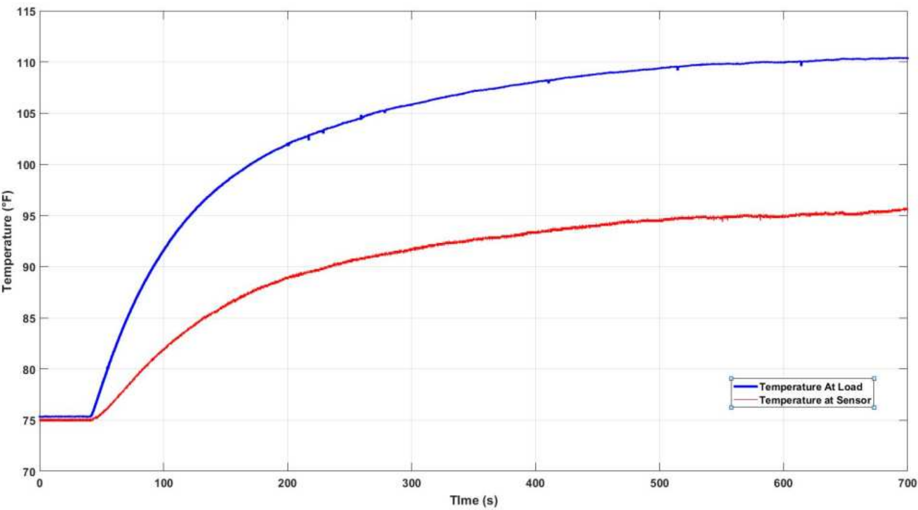

図 25. System Load Temperature vs Temperature Sensor Near Load

After taking the difference between the two curves in 図 25, the differential can be modeled with a poly-fit curve in MATLAB. This curve allows the input reading from the sensor to automatically be converted into the correct value in firmware. This value can be used as a secondary check for relating the temperature of the load to the sensed current, which is useful for system calibration when the system is conditioning air outside of normal temperatures (that is, turning on the heat when the internal home temperature is 40°F). The load temperature to sensor relationship can be expressed as:

$$y = -0.12z^4 - 0.14z^3 - 0.41z^2 + 1.9z + 14 \quad (18)$$

Copyright © 2018, Texas Instruments Incorporated

where:

$$z = \frac{Temp - 91}{5.6}$$

Copyright © 2018, Texas Instruments Incorporated

図 26 graphically represents this relationship.

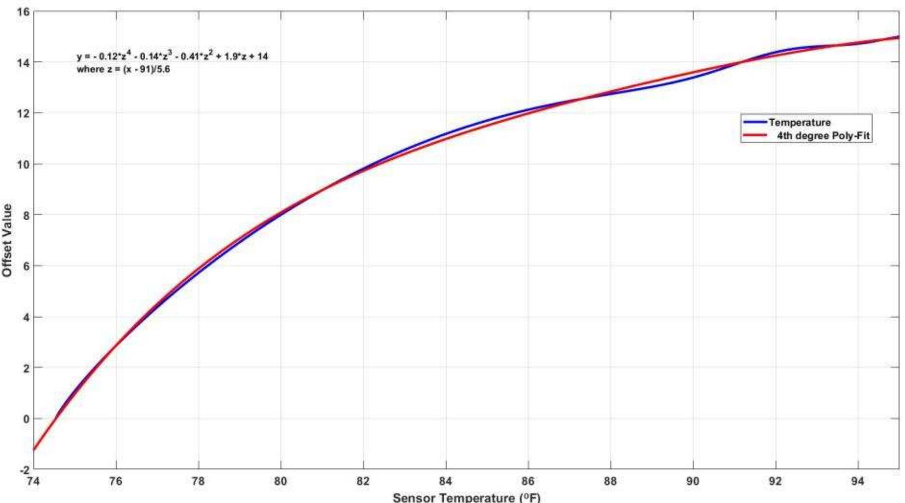

図 26. Load to Sensor Offset Curve

For this algorithm, the emphasis is placed on using the involved sensors together with logic to obtain an accurate estimate of the ambient temperature. For more information on the logic portion of this algorithm, see 図 29. In this case, characterize this algorithm for a cooling cycle. The same can be done for a heating cycle using the same method.

The INA230 gives the user the ability to know the state of the system at any time. Assuming for simplicity that there are only two current states, a 250-mA "on" state and an arbitrary "off" state current, this value can act as a logic mechanism for the remainder of the temperature offset process. Using the INA230's high accuracy, the designer can implement an infinite combination of current schemes if desired.

"Latch" in the corrected surface sensor 1 value using the algorithm described in 2.4.6.2 to have a baseline value for comparison. For this comparison, assume two additional items:

1. The temperature "latched" is the upper reference point to determine the ambient temperature. Because a cooling cycle is initiated, the temperature should not continue to increase once the load has reached a steady-state temperature.
2. The temperature rise of the surface sensor with respect to load influence reaches a particular steady-state value based on the ambient temperature change.

TIDUDO1 翻訳版 — 最新の英語版資料 http://www-s.ti.com/sc/techlit/TIDUDO1
Copyright © 2018, Texas Instruments Incorporated

図 27 shows an example.

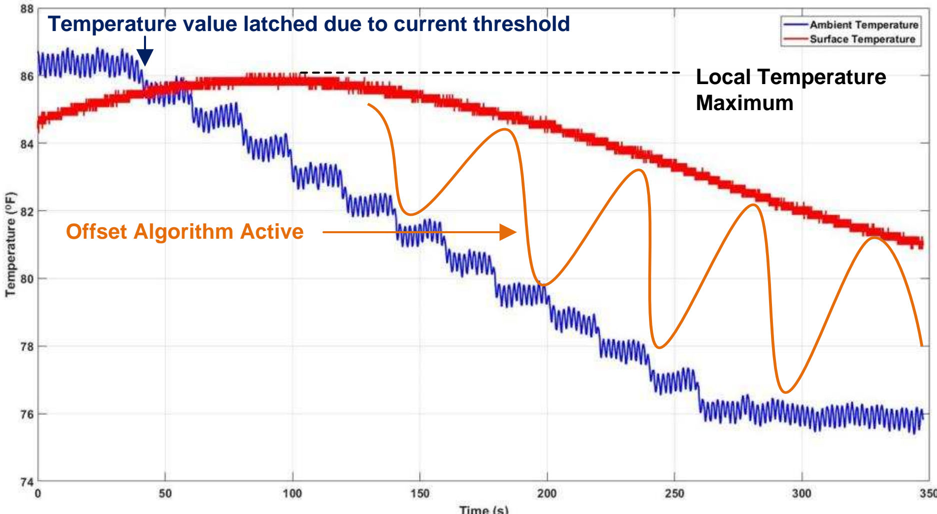

図 27. TMP235 Sensor 1 vs Ambient Temperature

From this time-based steady-state acquisition, the ambient temperature can be estimated. The device is placed in a thermal chamber regulated at a temperature between 21°C and 28°C, where the maximum temperature given by the temperature sensor on the bottom of the PCB is noted. From this data, MATLAB is used for basic fitting of the data, as shown in 図 28.

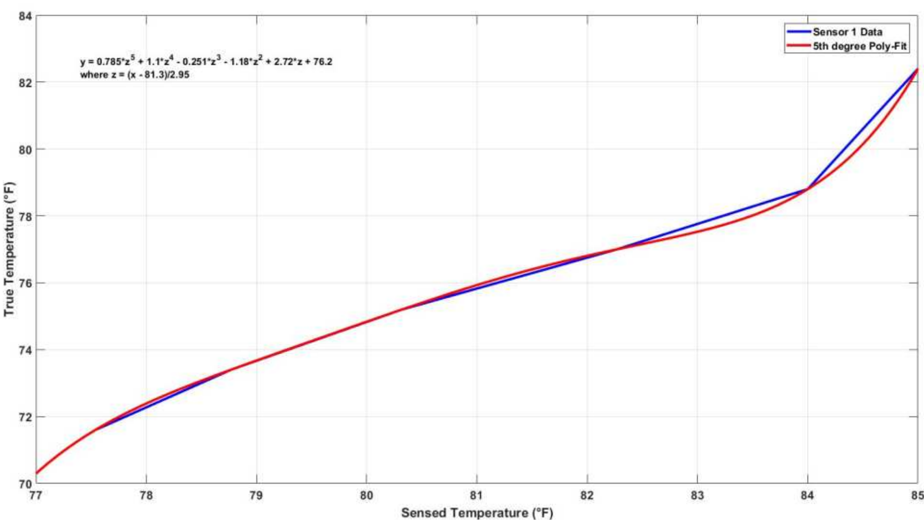

図 28. Surface Temperature Peak Value vs Ambient Temperature

From this poly-fit, the resulting curve equation is defined as:

$$y = 0.785z^5 + 1.1z^4 - 0.251z^3 - 1.18z^2 + 2.72z + 76.2 \quad (19)$$

where:

$$z = \frac{Temp - 81.3}{2.95}$$

TIDUDO1 翻訳版 — 最新の英語版資料 http://www-s.ti.com/sc/techlit/TIDUDO1
Copyright © 2018, Texas Instruments Incorporated

式 19 is used in conjunction with the logic flow shown in 図 29 to obtain an approximated ambient temperature related to the sensor reading.

INA230 Current Acquisition

No

Current Threshold Met

Yes

Poly-Fit Offset Value Computation

Acquire Sensor 1,2 Temperature Values

Yes

+

Calibrate Load Temp

Sensor 2 to Load Offset Correction Poly-Fit

No

Temperature or Calculated Max for Current Value

Latch Sensor 1 Value

Local Maximum Value Detect

To Terminal

Values Match

図 29. Flow Chart of Current and Temperature Monitoring Algorithm

For this method, the load temperature plays an important role in the resulting temperature increase sensed from the temperature sensor on the bottom of the PCB. Using a slight modification of 式 7 to account for the conductive heat transfer, the Joules per second delivered through the board to the temperature sensor is determined using 式 20:

$$q = \frac{\partial T \times A}{2\left(\frac{t_1}{k_1}\right) + 2\left(\frac{t_2}{k_2}\right) + 2\left(\frac{t_3}{k_3}\right) + \frac{t_4}{k_4}} \quad (20)$$

Using the values for the material used, FR4 Epoxy (k = 0.81) and copper (k = 385) in 式 21, along with the respective layer thickness and total area of the board and temperature range, this value is obtained, as shown in :

Copyright © 2018, Texas Instruments Incorporated

$$q(W) = \frac{(317.039\,K - 296.483\,K)\,K \times 6.68 \times 10^{-3} m^2}{2\left(\frac{3.556 \times E^{-5} m}{385 \frac{W}{m \times k}}\right) + 2\left(\frac{127 \times E^{-6} m}{0.81 \frac{W}{m \times k}}\right) + 2\left(\frac{3.607 \times E^{-5} m}{385 \frac{W}{m \times k}}\right) + \left(\frac{228.6 \times E^{-6} m}{0.81 \frac{W}{m \times k}}\right)}$$
$$q = 230.33 \frac{J}{s} \tag{21}$$

Using this data, the designer can determine an approximate heat dissipation value to the target sensor over time. Using this along with characterization of the differential in this value over ambient temperature variations can provide a very accurate model for thermal offset correction. For this design, this data is used as a secondary verification for the MATLAB simulations.

2.4.6.2 Two-Sensor Surface Temperature Sensing Method

This method is widely used in the HVAC industry for its simplicity and relatively good accuracy. As discussed in 2.4.3, there is a method for the specific placing of the temperature sensors. This method ensures a robust dynamic temperature range that can be used to determine the offset temperature. Due to how unique each thermostat design is, the designer must make algorithm adjustments accordingly.

For this method, the board is again characterized with respect to the target sensors being used in this algorithm. 図 30 shows the TMP235 output from a high temperature to an ambient satisfied temperature determined by the thermostat. This data can be compared to the change in internal temperature of the thermostat during a cooling cycle. The temperature is monitored during a test to mimic an actual cooling cycle from 88°F to 71°F. The surface temperature data can then be compared to the actual ambient temperature to establish a mathematical relationship. Because heat energy rises, the temperature variations seen in the plot coincide with different altitudes within the temperature chamber. In this case, the ambient temperature is measured at the return of the temperature chamber, which is located near the top of the instrument.

The dynamic temperature change is most closely related to the first temperature sensor located on the bottom of the board; therefore, this value is used as a baseline for determining the temperature offset within the system. The designer has the option to implement additional mathematical relationships to make temperature readings even more precise. The bottom sensor is chosen for simplicity in this case.

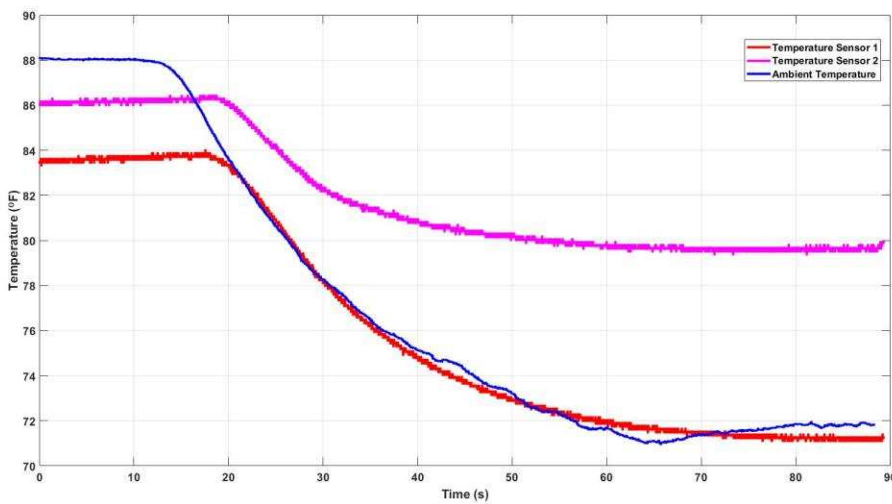

図 30. TMP235 Sensed Temperature vs Ambient Air Temperature

Copyright © 2018, Texas Instruments Incorporated

From this data, a poly-fit model can be used to best fit the temperature differential between the ambient and the sensor temperature. First, the differential between the true ambient temperature and the bottom layer temperature sensor is derived. This sensor is chosen due to the lack of influence this sensor receives from the heat load. Once plotted, red in 図 31, the data curve undergoes a poly-fit transformation, which best represents the curve mathematically. 式 22 is then used to compute the offset value from the true ambient temperature under the previously defined testing conditions.

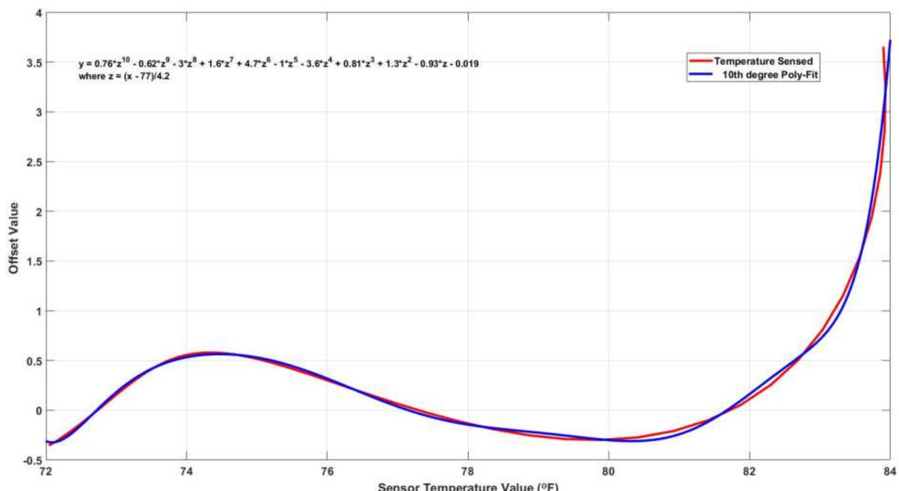

図 31. Sensor 1 vs Ambient Temperature Curve

$$y = 0.76z^{10} - 0.62z^{9} - 3z^{8} + 1.6z^{7} + 4.7z^{6} - 1z^{5} - 3.6z^{4} + 0.81z^{3} + 1.3z^{2} - 0.93z - 0.019 \quad (22)$$

where:

$$z = \frac{Temp - 77}{4.2}$$

式 22 can then take the initial temperature reading from the bottom sensor and convert it into an estimated ambient temperature. 式 22 is based on the particular test conditions of the system and the most accurate poly-fit available. The designer ultimately decides on what accuracy is required and the processing power limit with respect to high degree polynomials. If needed, slight addition or subtraction arithmetic can be preformed on the results to fine tune a unique system or add an anticipator function.

2.4.6.3 Convective Heat Sensing Method

This method takes advantage of the five LMT84 sensors placed on the PCB, which is slightly elevated from the surface of the board. The temperature sensed form these sensors are based on the heat being dissipated from the board to the thermostat case through convection. Before deriving a relationship between the heat transfer measured from the sensors and the outside true ambient temperature, the behavior of the system is again captured for analysis. 図 32 shows the resulting temperature readings from the convective temperature sensors and the ambient air during a system cooling cycle. As expected, the temperature of each LMT84 decreases with the ambient temperature and becomes more varied as the temperature decreases.

TIDUDO1 翻訳版 — 最新の英語版資料 http://www-s.ti.com/sc/techlit/TIDUDO1
Copyright © 2018, Texas Instruments Incorporated

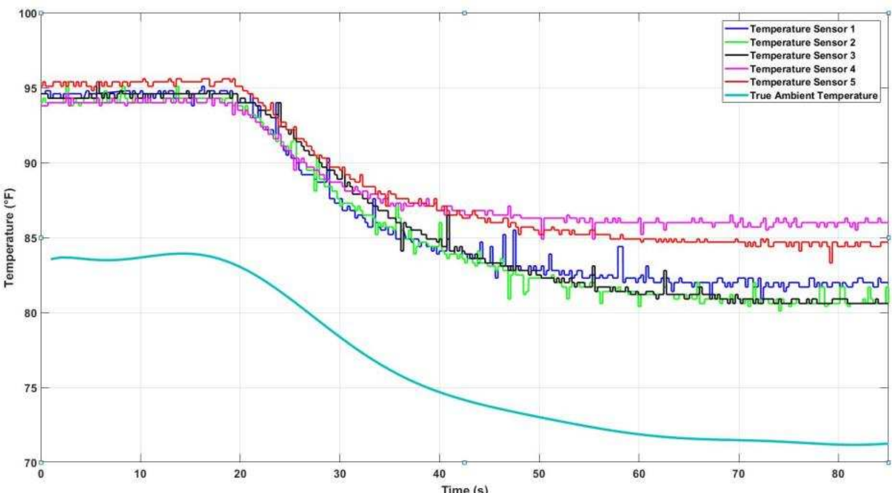

図 32. LMT84 Convective Sensing Output vs True Ambient Temperature

From this data, sensor 2 is used as a baseline for the prediction process because it is on average the closest temperature to ambient. The remaining sensor values are averaged to estimate the overall convective heat transfer influence across the PCB during a system cycle to sensor 2. Once calculated, this value is compared to the data from sensor 2 for a differential value, which is then subtracted from the sensor 2 reading to offset any heat sensed from the remaining sensors. In this case, all averages from the remaining sensors indicate a higher temperature reading than that of the main sensor. Therefore, there is no need to consider adding any offset to the readings in firmware, only subtracting.

After completing these steps, the results are characterized graphically as shown in 図 33.

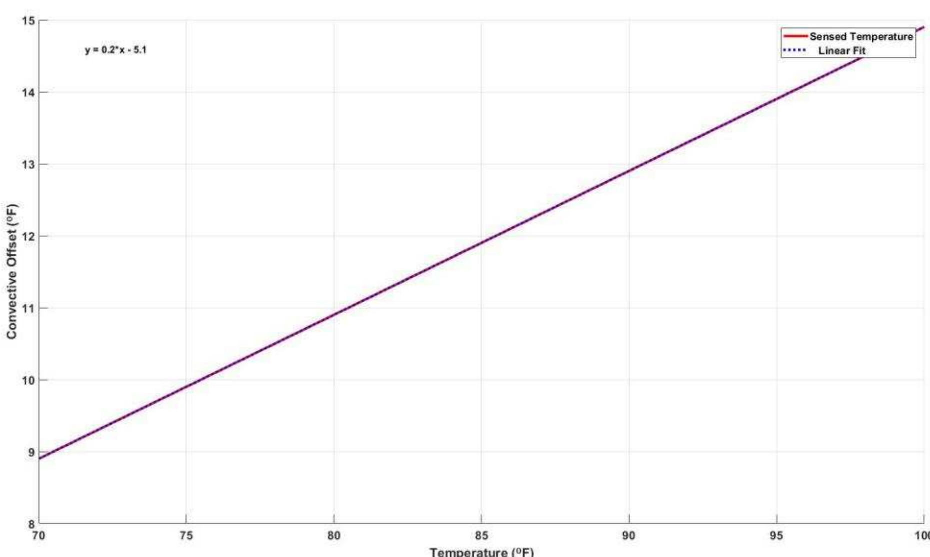

図 33. Poly-Fit Curve of Convective Sensing Offset Value

From the extracted polynomial model:

$$y = 0.2x - 5.1 \quad (23)$$

Copyright © 2018, Texas Instruments Incorporated

式 23 is implemented in firmware with the temperature variable coming from the combination of all PCB sensors. The resultant value is then subtracted from the sensed temperature to remove any offset due to the internal heat generation. Once corrected, this value can be relayed to the user and implemented as an accurate temperature threshold for a typical HVAC cycle.

Copyright © 2018, Texas Instruments Incorporated

3 Hardware, Software, Testing Requirements, and Test Results

3.1 Required Hardware and Software

The following sections describe the quickest way to get the reference design board up and running for evaluation.

3.1.1 Hardware

図 34 shows the design board. This board is meant to be used with TI's wireless CC series LaunchPad development kits and connected with the use of the integrated board headers. The board also has multiple jumper pin placements to allow the user to isolate specific devices for testing as well as obtain the power consumption values from the board. 表 8 shows the main jumpers used in this reference design along with their respective components being supplied power.

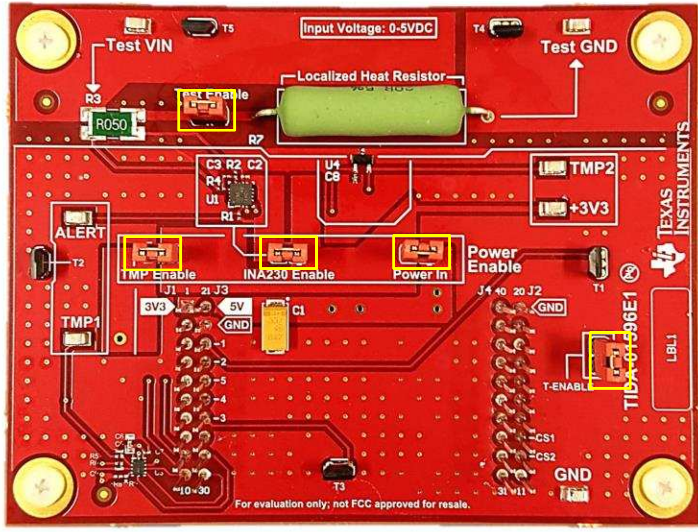

図 34. TIDA-01596 Power Jumper Locations

表 8. Power Jumper Configuration and Function

JUMPER	FUNCTION
TEST ENABLE	Enables power through the power resistor for heat generation
TMP ENABLE	Provides power to the TMP235 devices and the discrete nanopower sensor monitor
INA230 ENABLE	Provides power to the INA230
POWER IN	Provides main power to the software controlled section of the board
T-ENABLE	Power for the discrete convective LMT84 sensors

After ensuring the jumpers are correctly placed, the design board can be placed on the CC3220 LaunchPad through the use of the headers provided on both boards.

TIDUDO1 翻訳版 — 最新の英語版資料 http://www-s.ti.com/sc/techlit/TIDUDO1
Copyright © 2018, Texas Instruments Incorporated

3.1.2 Software

The following section describes the process for bringing the design firmware online and deployed to the CC device.

First, install the firmware from TI.com. After obtaining the file, import it into Code Composer Studio™ (CCS) as a zipped project. Once the code is loaded successfully, compile and build it. 図 35 shows the building of the design firmware in CCS.

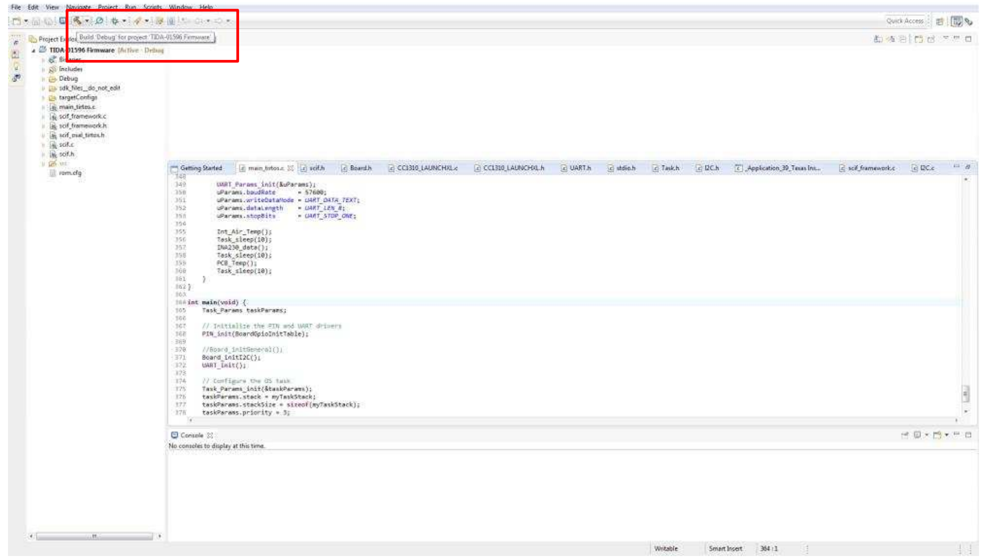

図 35. Building the TIDA-01596 Code in CCS

Copyright © 2018, Texas Instruments Incorporated

Next, ensure the board is firmly connected to the CC device through the USB connector. This connection allow the deployment of the firmware to the device memory. 図 36 shows the proper setup for firmware deployment of the firmware. The power connection to the test circuit are not necessary for this step, but are shown for user reference.

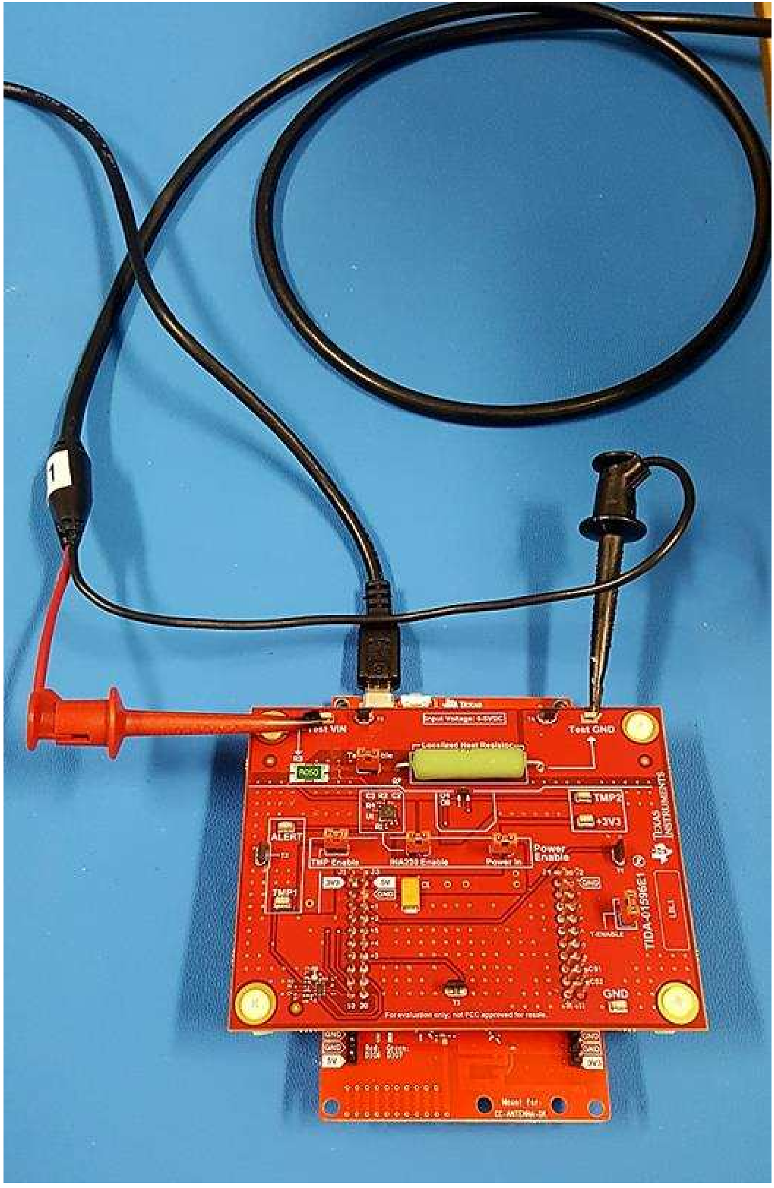

図 36. Board Setup for Firmware Deployment

Copyright © 2018, Texas Instruments Incorporated

After the firmware is successfully built and the board is properly connected to the computer, it is next debugged and deployed to the target device. 図 37 shows this process.

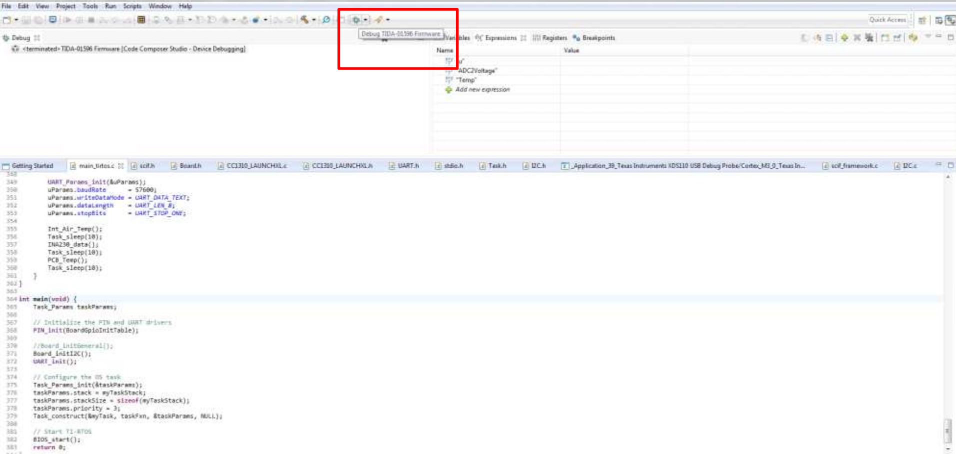

図 37. Debugging and Deploying the TIDA-01596 Firmware

Once the firmware is successfully deployed to the device, the board is ready to start taking temperature and current measurements. To do this, a program such as PuTTY is used for a serial connection to the COM port used by the device. For the computer used in this testing, the following represents the setting for opening the serial terminal from putty. The baud rate, defined in the software, is required along with the port attached to the CC3220 device. If unknown, these settings can be found through the computers device manager program. In this case, the serial port is set to 30 with a baud rate of 57600.

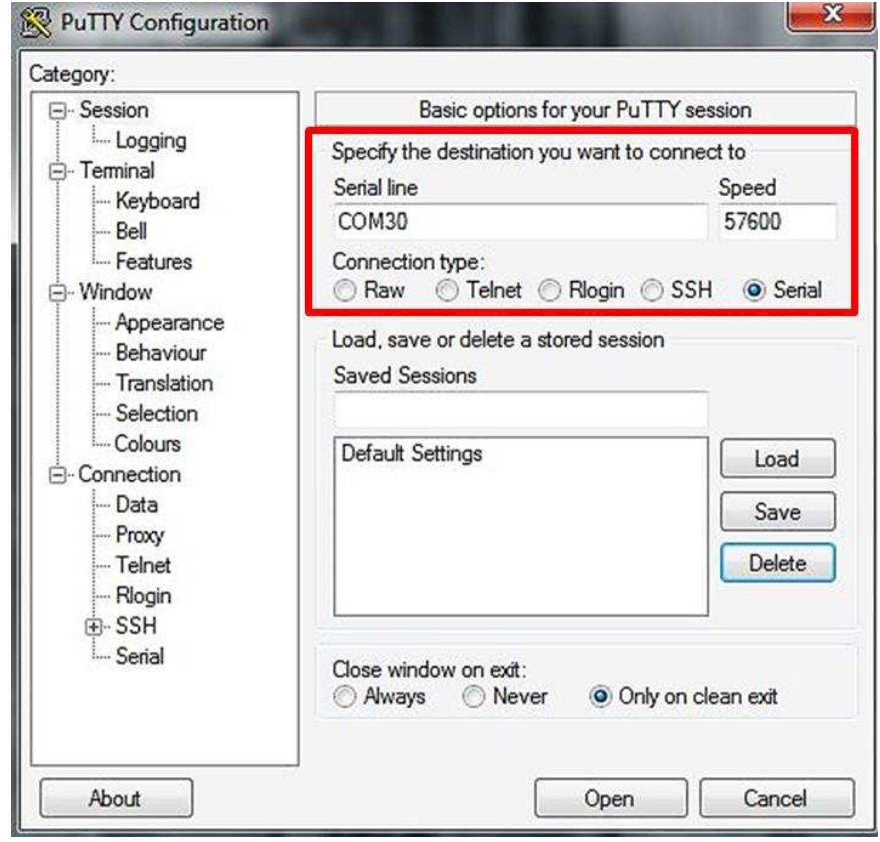

図 38. PuTTY Serial COM Port Settings

TIDUDO1 翻訳版 — 最新の英語版資料 http://www-s.ti.com/sc/techlit/TIDUDO1
Copyright © 2018, Texas Instruments Incorporated

After entering the shell, the device begins printing values to the screen, as shown in 図 39. These values are used for acquiring data and can be commented out or added to the corrected values for analysis by the user.

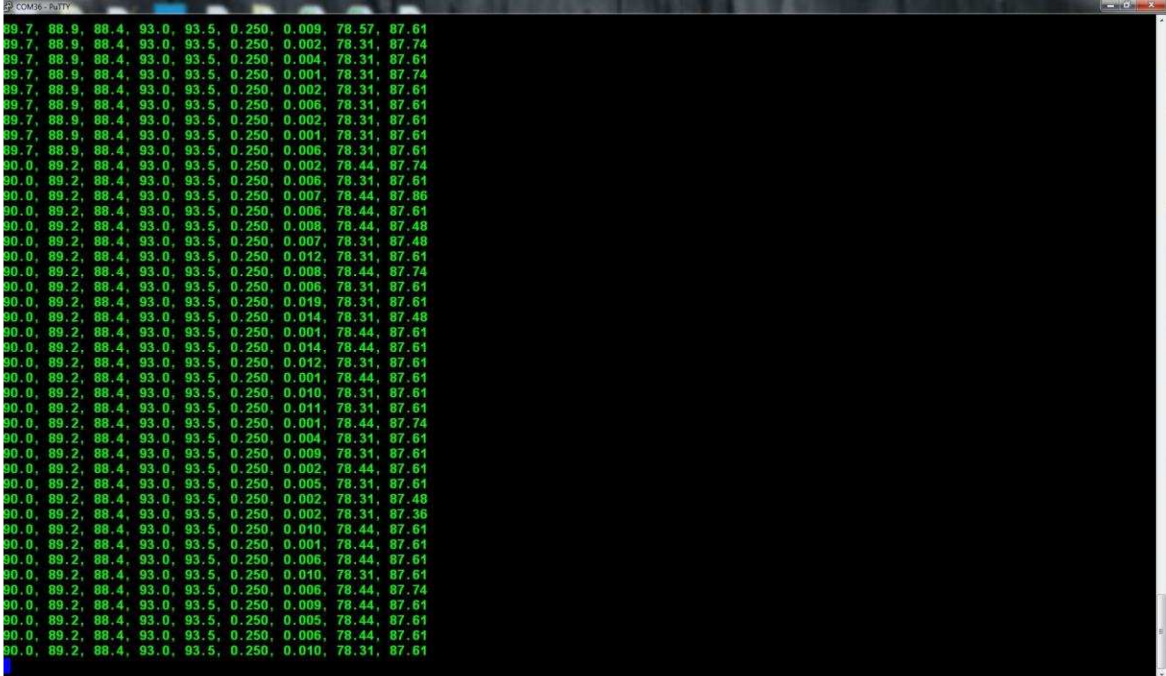

図 39. Screenshot of UART Sensor Data Output

The order and visibility of each sensor value shown in 図 39 can be modified by the user as needed for specific testing. Additionally, these values can be modified to only show corrected temperatures.

Copyright © 2018, Texas Instruments Incorporated

3.2 Testing and Results

The following sections describe the setup used for testing as well as their respective results. Some of the test setups are not followed by a unique result in the results section; these results are detailed in the 2.4.

3.2.1 Test Setup

, 図 40 shows the setup used for the initial testing of the board with respect to sensor readings. A DC power supply is connected to the VIN and GND test points of the test load section of the board. The board is connected to a computer through the LaunchPad located on the bottom of the design and connected to the headers. The DC power supply slowly increases up to the limit value of 5 V, and the sensor values are acquired for analysis. The poly-plane and trace resistance are also verified with the use of a digital multimeter (DMM) in place of the DC power supply.

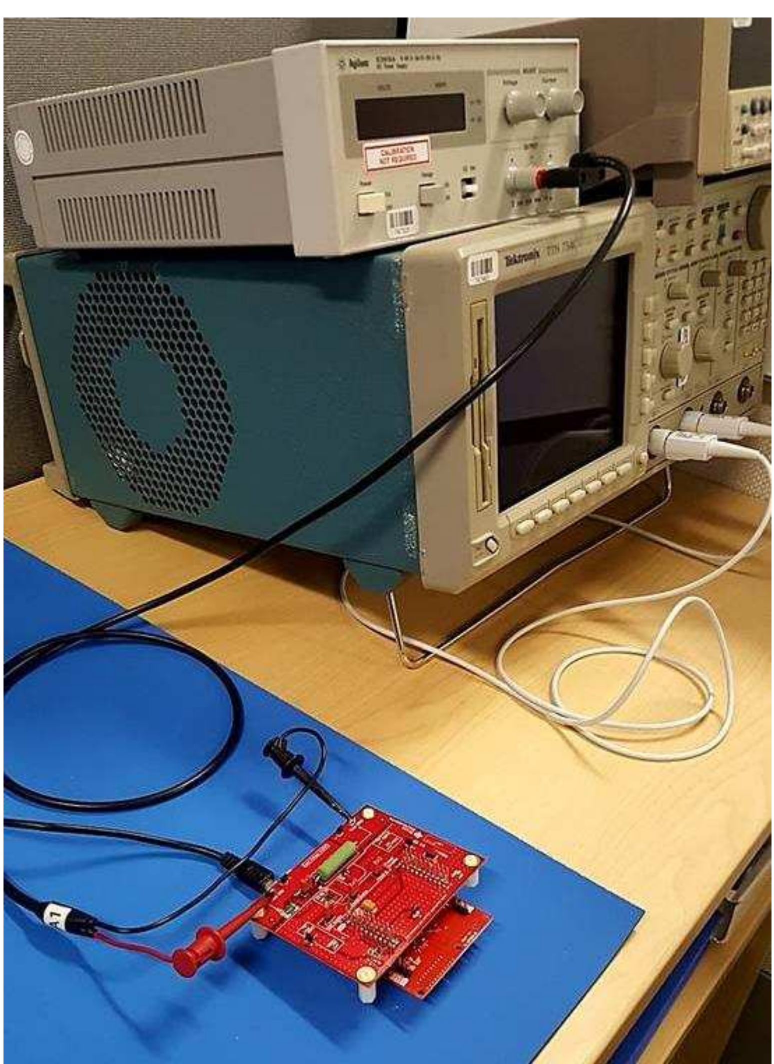

図 40. Test Setup of Initial Sensor Data Acquisition and Circuit Resistance

Copyright © 2018, Texas Instruments Incorporated

To gain an accurate surface temperature value for the load resistor used in this reference design, a clamp-style thermocouple is placed on the load resistor as shown in 図 41. The thermocouple is attached to a handheld meter with the ability to measure temperature through the k-type connector port of meter. The voltage level is then swept from 0 V to 5 V in 100-mV increments and the resulting temperature recorded. 図 23 shows these results.

図 41. Test Setup of Ambient Load Temperature

Copyright © 2018, Texas Instruments Incorporated

Using the handheld meter and the clamp-style thermocouple again, a thermostat case is placed over the design board and the CC3220 LaunchPad. In this test, the thermocouple senses the ambient temperature while the internal sensors on the design board are monitored through the UART interface as described in 図 38. This testing is done in a lab environment without using the thermal chamber. The DC supply clamps used in the previous testing setups are not shown here; the clamps are replaced by a direct wire connection to allow a better fit inside the thermostat case (not shown).

図 42. Load Offset From Ambient Test Setup In Thermostat Case

図 43 shows the main testing setup used in the temperature offset algorithm. For this testing, a Test Equity Half-Cube temperature chamber is used as the environment for testing. This allows for temperature variations required for measuring resistance variation as well as characterizing the offset curve for a typical HVAC cooling cycle.

The board is placed in the thermostat case as described previously. the launchpad is removed from the backside of the board to remove any temperature influence from the launchpad to the bottom temperature sensor on the test board. Jumper wires are used to connect the main component power supplies as well as the I2C communication lines. The thermocouple is used to verify the ambient air temperature near the test device against the reading on the thermal chamber. A second 2-wire thermocouple is placed inside the case and placed in contact with the test load. This thermocouple is attached to an Agilent DMM, remotely controlled by LabVIEW™.

TIDUDO1 翻訳版 — 最新の英語版資料 http://www-s.ti.com/sc/techlit/TIDUDO1
Copyright © 2018, Texas Instruments Incorporated

図 43. Test Setup of Temperature Chamber System

図 44 shows the front panel of the LabVIEW environment used for data acquisition. The thermistor value is translated into a DC voltage through the use of a Fluke Type-K to banana plug adapter, which outputs 1 mV per degree Fahrenheit. With respect to sampling settings, the DMM is set up to take 10 samples per trigger event with 10 trigger events per second. This rate enables high resolution with respect to load temperature changes during the test cycle.

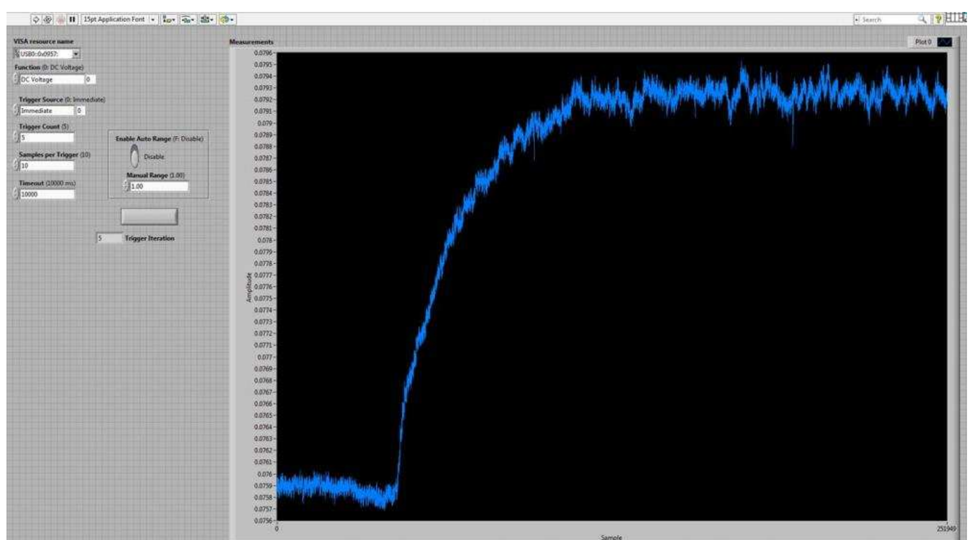

図 44. LabVIEW™ Test Panel for Thermistor Data Acquisition

Copyright © 2018, Texas Instruments Incorporated

The LabVIEW front panel outputs the data in graphical form for user analysis. This data is also exported into Excel® for further data analysis in MATLAB as outlined in 2.4.6. The user has the ability to increase or decrease the sampling resolution through the front panel triggering options shown in 図 44.

3.2.2 Test Results

The following section describes the test results of the temperature offset correction using the setup shown in 図 43. For preliminary results used in the development of offset correction algorithms, see 2.4.6.

3.2.2.1 Simulation Verification Results

When developing an algorithm to correct offset due to localized thermostat heat generation, one of the most important things is accuracy in the simulation model. With a highly accurate simulation model, the system behavior can be modeled for different conditions with high confidence in predicting the resulting offset generated. 図 45 compares the MATLAB simulation results to the actual results obtained through design testing. From 図 46, the load resistor reaches a temperature value of 43.25°C, or 109.85°F, at 1424 seconds. In comparison, at approximately the same time on the simulation, the temperature is 43.19°C, or 109.742°F. These results yield a simulation to an actual test error of 0.098%. This error indicates that the MATLAB model is very accurate with respect to the actual board testing and can be used by the designer with multiple heat loads to obtain similar results.

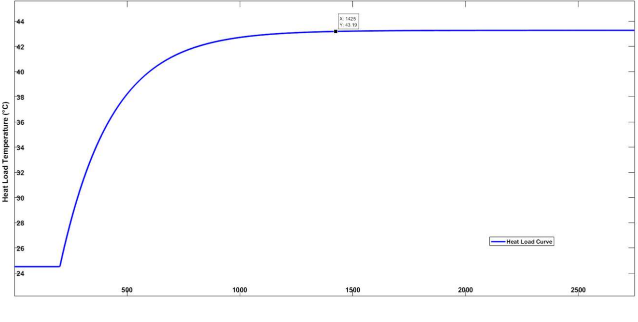

図 45. MATLAB Simulation of Load Heat Curve

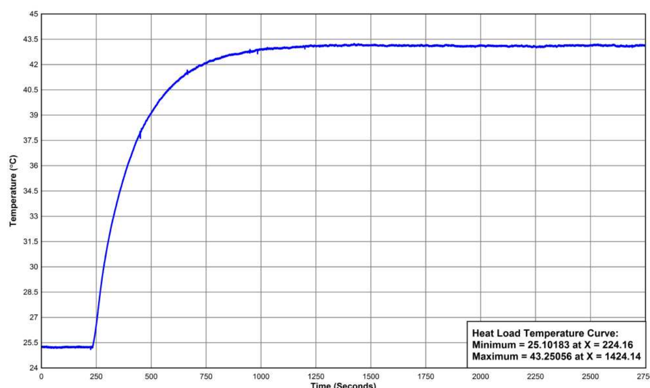

図 46. TIDA-01596 Measured Heat at 250 mA

Taking the differential from the heat load shown in 図 46 and the true ambient temperature provides a comparison of the offset values from the load resistor to the ambient air. These results are proportional to the temperature curves shown and have an approximated error of 0.8%. From this data, for an ambient temperature of 75°F, the internal offset directly relates to these curves. For variations with respect to the ambient temperature, the simulation yields a linear relationship with the load offset temperature and the ambient temperature adjustment.

TIDUDO1 翻訳版 — 最新の英語版資料 http://www-s.ti.com/sc/techlit/TIDUDO1
Copyright © 2018, Texas Instruments Incorporated

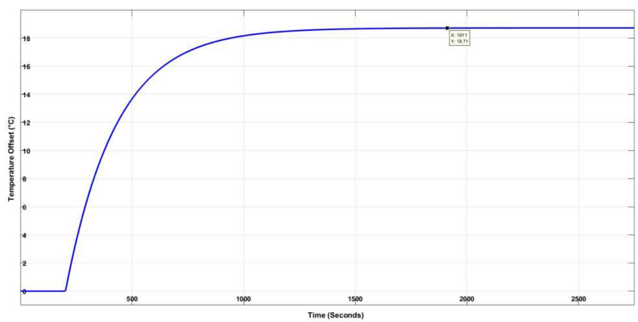

図 47. MATLAB Simulation of Thermal Offset From Load To Ambient

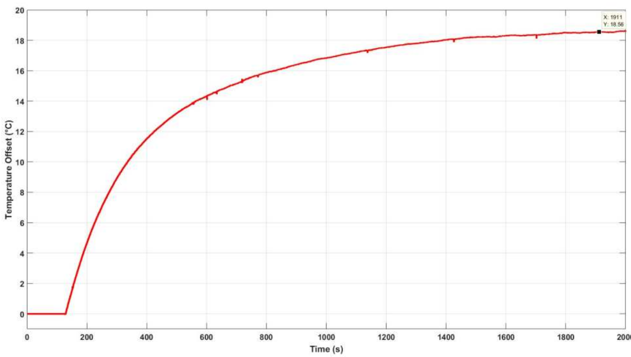

図 48. TIDA-01596 Measured Thermal Offset From Load to Ambient

3.2.2.2 Thermal Offset Algorithm Accuracy Verification

The following subsections provide an analysis of the temperature sensor data after implementing the thermal offset algorithms. These results are based on thermal chamber testing, which varies greatly from that of an actual household environment; however, the process will be the same.

3.2.2.2.1 Results of Current and Temperature Monitoring Algorithm

図 49 shows the results of the algorithm accuracy when using the temperature sensor and current sensing in conjunction. In the plot, the red line represents the load temperature, the blue represents the ambient temperature of the thermal chamber, and the pink line represents the output temperature of the algorithms. The constant temperature in the beginning is based off the latch function as stated in 2.4.6.1. Assuming the HVAC system is set to run a cooling cycle, the last corrected temperature before the thermostat goes into an active state is recorded as the upper limit of the thermal prediction. Using 式 20 along with the characterized heat load behavior of this system, a load resistor temperature is used to trigger the algorithm. Once the temperature has reached 100°F at the load, the heat dissipation becomes influential enough to put the corrected reading within the bounds of the algorithm.

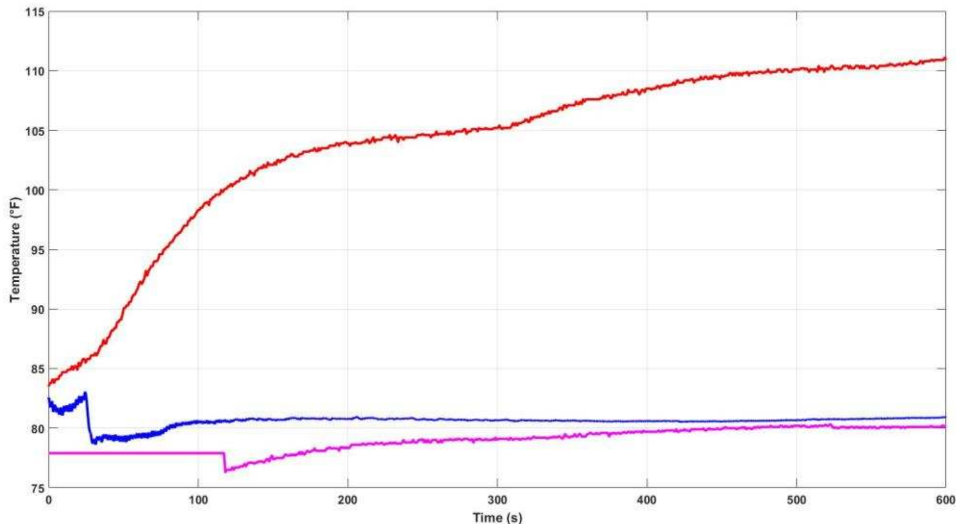

図 49. Results of Current and Temperature Monitoring Algorithm

Copyright © 2018, Texas Instruments Incorporated

This trigger point causes the algorithm to go into action once the load reaches 100°F. The temperature briefly dips before approaching the true ambient temperature due to the remainder of heat energy the sensor must detect to reach the fully correct value. At this point, the load is approaching 112°F. Further analysis shows that after the initial dip in approximated temperature is on average < 1°F, or < 0.56°C, from the true ambient temperature in the thermal chamber. The correction algorithm increases in accuracy as the cooling cycle continues, providing even higher accuracy near the assumed cycle end time of 10 minutes.

3.2.2.2.2 Results of Surface Temperature Sensor Algorithm

図 50 shows the resulting temperature correction using the surface temperature offset algorithm. The temperature is held at approximately 85°F before being reduced to 74°F. Due to the behavior of the thermal chamber, the offset algorithm integrates an additional offset anticipator, which resets the temperature initially to account for the accelerated temperature drop. The temperature decrease with respect to the ambient reading decreases by step values to decrease the effects of this rapid temperature change. This temperature change can be removed by the designer for testing in an actual household environment.

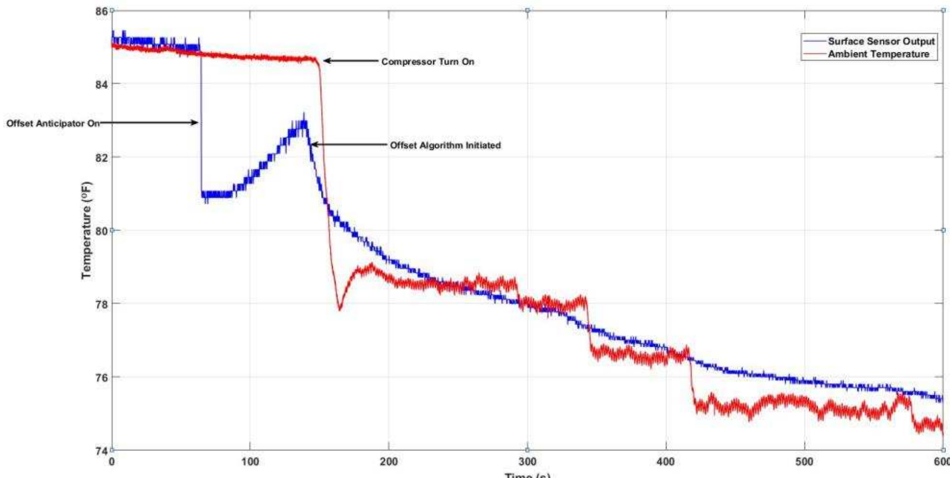

図 50. Results of Surface Sensor Offset Correction

Once the thermal chamber compressor turns on, the temperature begins to decrease to 79°F before being stepped down to 74°F. The offset algorithm initially increases before conforming to the actual ambient temperature using the developed mathematical relationship between the two. As the temperature continues to decrease, the offset curve the accuracy becomes greater. This increase is expected due to the characterization range of the temperature sensor. Further analysis of the data shows that the offset from the true ambient temperature to the surface temperature is on average < 1°F, or < 0.56°C, with respect to the differential between the two from 89°F to the target set temperature of 74°F. This data is acquired over a 10-minute period, the assumed average cycle time per hour.

The designer can increase the resolution of the offset algorithm to increase offset prediction accuracy. The mathematical relationship is based on a dynamic change during a typical cycle. This can be simplified by modeling the system in a static state or developing the algorithm in true environmental conditions; in this case, the temperature dynamics are much less significant in the modeling.

Copyright © 2018, Texas Instruments Incorporated

3.2.2.2.3 Results of Convective Temperature Sensing Algorithm

図 51 shows the convective sensing results. As mentioned previously, there is a slight delay from the temperature change to the accurate temperature value. This delay is due to the thermodynamic delay from board heat absorption into the internal air, in addition to the rate of thermal change from the ambient environment to the internal cavity of the thermostat case.

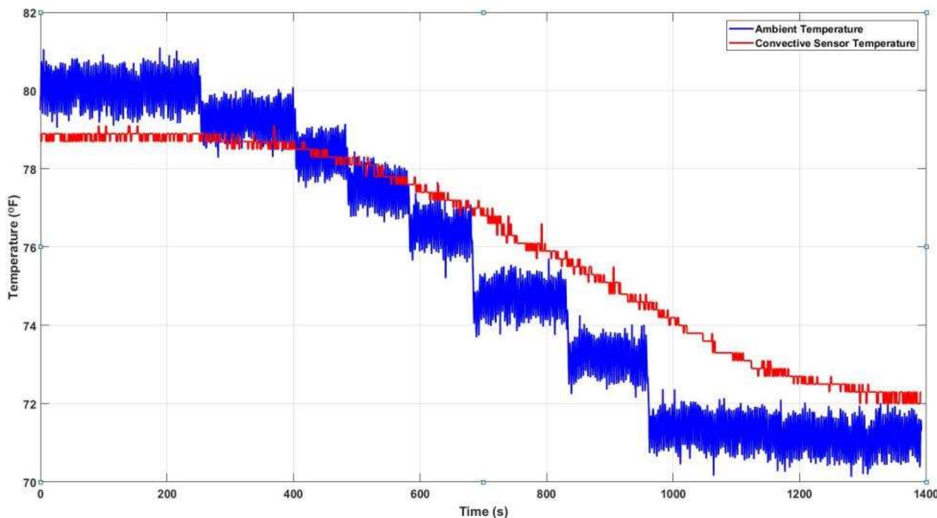

図 51. Results of Convective Temperature Offset Algorithm

For this test, the temperature is stepped down incrementally from approximately 86°F to 76°F. Further analysis of the data shows that the average difference between the actual temperature and that given by the offset correction algorithm is about 0.667°F or 0.372°C. This algorithm provides a high level of accuracy based on convective heat transfer sensing while maintaining low cost. Thermistors can also be used in this application with similar results based on the accuracy of the component used. The required accuracy is left for the designer to decide. The algorithm also provides slightly more accurate results when using more than one sensor, along with the derived methods for ambient temperature sensing.

3.2.2.3 Board Current Consumption

表 9 shows the resulting measurements for both total power consumption of the board, neglecting the CC3220 power from the computer. These results target each respective device or device group to provide an accurate overview of each sections contribution to the overall power consumption. These results also can be used to derive the efficiency of the layout based on the value differential between each separate group and the total current consumption measured at the main power input to the board.

表 9. TIDA-01596 Current Consumption Results

MEASURED PARAMETER	AVERAGE VALUE OVER TESTED TEMPERATURE RANGE
Total current	469.64 µA
LMT84 network	24.568 µA
TMP235 sensors and ADS7142	142.56 µA
INA230	302.48 µA
Efficiency	99%

Copyright © 2018, Texas Instruments Incorporated

4 Design Files

4.1 Schematics

To download the schematics, see the design files at TIDA-01596.

4.2 Bill of Materials

To download the bill of materials (BOM), see the design files at TIDA-01596.

4.3 PCB Layout Recommendations

The key to estimating the ambient temperature accurately is to ensure an optimized PCB layout. Pay attention to where the sensors are placed as well as ensure a good heat dissipating plane near the heat load and farther from the main temperature sensing device.

4.3.1 Layout Prints

To download the layer plots, see the design files at TIDA-01596.

4.4 Altium Project

To download the Altium project files, see the design files at TIDA-01596.

4.5 Gerber Files

To download the Gerber files, see the design files at TIDA-01596.

4.6 Assembly Drawings

To download the assembly drawings, see the design files at TIDA-01596.

5 Software Files

To download the software files, see the design files at TIDA-01596.

6 Related Documentation

1. Texas Instruments, *CC3220 SimpleLink™ Wi-Fi® Wireless and Internet-of-Things Solution, a Single-Chip Wireless MCU Data Sheet*
2. Texas Instruments, *TMP235 Low-Power, High-Accuracy Analog Output Temperature Sensors Data Sheet*
3. Texas Instruments, *High- or Low-Side Measurement, Bidirectional CURRENT/POWER MONITOR with I2C™ Interface Data Sheet*
4. Texas Instruments, *ADS7142 Nanopower, Dual-Channel, Programmable Sensor Monitor Data Sheet*
5. Texas Instruments, *LMT84 1.5-V, SC70/TO-92/TO-92S, Analog Temperature Sensors Data Sheet*

6.1 商標

E2E, BoosterPack, MCU LaunchPad, SimpleLink, Internet-on-a-chip, SmartConfig, Code Composer Studio are trademarks of Texas Instruments.
Arm, Cortex are registered trademarks of Arm Limited (or its subsidiaries).
Bluetooth is a registered trademark of Bluetooth SIG, Inc.
Excel is a registered trademark of Microsoft Corporation.
LabVIEW is a trademark of National Instruments.
MATLAB is a registered trademark of The MathWorks, Inc.
Wi-Fi, Wi-Fi CERTIFIED, Wi-Fi Direct are registered trademarks of Wi-Fi Alliance.

Copyright © 2018, Texas Instruments Incorporated

すべての商標および登録商標はそれぞれの所有者に帰属します。

7 About the Author

BRIAN DEMPSEY is a systems designer at Texas Instruments, where he is responsible for developing reference design solutions for the industrial and building automation segment. Brian brings to this role his extensive experience in the HVAC industry, along with his experience with mixed signal systems design. Brian earned his bachelor of science in electrical engineering (BSEE) from Texas A&M University in College Station, TX. Brian is a member of the Institute of Electrical and Electronics Engineers (IEEE).

Copyright © 2018, Texas Instruments Incorporated

TIの設計情報およびリソースに関する重要な注意事項

Texas Instruments Incorporated ("TI")の技術、アプリケーションその他設計に関する助言、サービスまたは情報は、TI製品を組み込んだアプリケーションを開発する設計者に役立つことを目的として提供するものです。これにはリファァレンス設計や、評価モジュールに関係する資料が含まれますが、これらに限られません。以下、これらを総称して「TIリソース」と呼びます。いかなる方法であっても、TIリソースのいずれかをダウンロード、アクセス、または使用した場合、お客様(個人、または会社を代表している場合にはお客様の会社)は、これらのリソースをここに記載された目的にのみ使用し、この注意事項の条項に従うことに合意したものとします。

TIによるTIリソースの提供は、TI製品に対する該当の発行済み保証事項または免責事項を拡張またはいかなる形でも変更するものではなく、これらのTIリソースを提供することによって、TIにはいかなる追加義務も責任も発生しないものとします。TIは、自社のTIリソースに訂正、拡張、改良、およびその他の変更を加える権利を留保します。

お客様は、自らのアプリケーションの設計において、ご自身が独自に分析、評価、判断を行う責任がお客様にあり、お客様のアプリケーション(および、お客様のアプリケーションに使用されるすべてのTI製品)の安全性、および該当するすべての規制、法、その他適用される要件への遵守を保証するすべての責任をお客様のみが負うことを理解し、合意するものとします。お客様は、自身のアプリケーションに関して、(1) 故障による危険な結果を予測し、(2) 障害とその結果を監視し、および、(3) 損害を引き起こす障害の可能性を減らし、適切な対策を行う目的での、安全策を開発し実装するために必要な、すべての技術を保持していることを表明するものとします。お客様は、TI製品を含むアプリケーションを使用または配布する前に、それらのアプリケーション、およびアプリケーションに使用されているTI製品の機能性を完全にテストすることに合意するものとします。TIは、特定のTIリソース用に発行されたドキュメントで明示的に記載されているもの以外のテストを実行していません。

お客様は、個別のTIリソースにつき、当該TIリソースに記載されているTI製品を含むアプリケーションの開発に関連する目的でのみ、使用、コピー、変更することが許可されています。明示的または黙示的を問わず、禁反言の法理その他どのような理由でも、他のTIの知的所有権に対するその他のライセンスは付与されません。また、TIまたは他のいかなる第三者のテクノロジまたは知的所有権についても、いかなるライセンスも付与されるものではありません。付与されないものには、TI製品またはサービスが使用される組み合わせ、機械、プロセスに関連する特許権、著作権、回路配置利用権、その他の知的所有権が含まれますが、これらに限られません。第三者の製品やサービスに関する、またはそれらを参照する情報は、そのような製品またはサービスを利用するライセンスを構成するものではなく、それらに対する保証または推奨を意味するものでもありません。TIリソースを使用するため、第三者の特許または他の知的所有権に基づく第三者からのライセンス、もしくは、TIの特許または他の知的所有権に基づくTIからのライセンスが必要な場合があります。

TIのリソースは、それに含まれるあらゆる欠陥も含めて、「現状のまま」提供されます。TIは、TIリソースまたはその仕様に関して、明示的か暗黙的かにかかわらず、他のいかなる保証または表明も行いません。これには、正確性または完全性、権原、続発性の障害に関する保証、および商品性、特定目的への適合性、第三者の知的所有権の非侵害に対する黙示の保証が含まれますが、これらに限られません。

TIは、いかなる苦情に対しても、お客様への弁護または補償を行う義務はなく、行わないものとします。これには、任意の製品の組み合わせに関連する、またはそれらに基づく侵害の請求も含まれますが、これらに限られず、またその事実についてTIリソースまたは他の場所に記載されているか否かを問わないものとします。いかなる場合も、TIリソースまたはその使用に関連して、またはそれらにより発生した、実際的、直接的、特別、付随的、間接的、懲罰的、偶発的、または、結果的な損害について、そのような損害の可能性についてTIが知らされていたかどうかにかかわらず、TIは責任を負わないものとします。

お客様は、この注意事項の条件および条項に従わなかったために発生した、いかなる損害、コスト、損失、責任からも、TIおよびその代表者を完全に免責するものとします。

この注意事項はTIリソースに適用されます。特定の種類の資料、TI製品、およびサービスの使用および購入については、追加条項が適用されます。これには、半導体製品(http://www.ti.com/sc/docs/stdterms.htm)、評価モジュール、およびサンプル(http://www.ti.com/sc/docs/sampterms.htm)についてのTIの標準条項が含まれますが、これらに限られません。

Copyright © 2018, Texas Instruments Incorporated
日本語版 日本テキサス･インスツルメンツ株式会社